# Extracting Damping Ratios Using Wavelets

by

**Jiun-Yan Wu**

Submitted to the Department of Civil and Environmental Engineering
in Partial Fulfillment of the Requirements for the Degree of

**MASTER OF ENGINEERING**
in Civil and Environmental Engineering

at the

**MASSACHUSETTS INSTITUTE OF TECHNOLOGY**

June 2001



Signature of Author

Department of Civil and Environmental Engineering
May 11, 2001

Certified by

Kevin Amaratunga
Assistant Professor of Civil and Environmental Engineering
Thesis Supervisor

Accepted by

Oral Buyukozturk
Chairman, Department Committee on Graduate Studies

# Extracting Damping Ratios Using Wavelets

by

**Jiun-Yan Wu**

Submitted to the Department of Civil and Environmental Engineering
on May 11, 2001 in partial fulfillment of the
requirements for the degree of
Master of Engineering in Civil and Environmental Engineering

## Abstract

The focus of this work is to evaluate the accuracy of methods for extracting damping ratios with respect to: three extraction methods, different damping ratios, added noisy data, separated modes and close modes.

To achieve this goal, a simulated analytical signal is analyzed by estimating the modal parameters. The simulated analytic signal is useful because the exact values are known and the characteristic of the FRF can be varied in order to observe how the accuracy of damping ratios is affected.

Results show that the Continuous Wavelet Transform method gives the most accurate estimations even for data corrupted by the noise. The Complex Exponential method presents better results in the cases with higher modes and higher damping ratios without the noise. Wavelet Packet method and Continuous Wavelet Transform method are more suitable in the cases for extracting lower damping ratios than those for higher damping ratios even for data corrupted by the noise. And in general, the estimation results are more accurate in the cases with separated modes than those with close modes.

**Thesis Supervisor: Kevin Amaratunga**
**Title: Assistant Professor of Civil and Environmental Engineering**

# Acknowledgments

To Prof. Kevin Amaratunga, who gave timely and thoughtful advice to help me clarify my thoughts and direction.

To all M.Eng. classmates, especially thanks to members in the I-Campus, for helping me make it through "the best year of my life".

To my parents for their continued support and encouragement through these challenging years.

And to my beloved wife, Lan-Ting Chen, for encouraging and giving me strength to do what I had to do. She brought me more love and strength to my life.

# Table of Contents

# List of Figures

# List of Tables

# Chapter 1
# Introduction

## 1.1 Problem Statement

Damping is a mechanism that dissipates vibration energy in dynamic systems. Its value is very important for the design and analysis of vibration structures because the dynamic response of structures and the transmission of vibrations to the surroundings are critically determined by the damping mechanism. In general, structural damping can be classified either as hysteretic or viscous. Hysteretic damping arises from microstructural phenomena and is characterized by material properties. Viscous damping is proportional to the magnitude of the velocity, and opposite to the direction of motion. But in practice, the concept of equivalent viscous damping is used to model the overall damped behavior of the system as being viscous. In this thesis, the damping ratio, $\zeta$ or fraction of critical damping is used to describe viscous damping.

Once the structure is modeled, the stiffness and mass distributions are quite well determined, but there is great uncertainty regarding the energy dissipating mechanism provided by the damping distributions of the structure because they are the most sensitive to noise, measurement errors, inadequate excitation, etc.

A lot of work has being devoted to the development and improvement of techniques for measuring damping values. Those techniques can be classified into time domain methods, which are based on the impulse response function (IRF) and frequency domain methods, which are based on the frequency response function (FRF). A combined time-frequency approach can also be applied to estimate the damping of the system by using, for example, the Wigner-Ville distribution. Normally for real structures, the damping ratio ranges between 2 to 20% [1].

This thesis will present three different methods of extracting damping ratios for multi-degree-of-freedom (MDOF) systems. These are the Complex Exponential Method (CEM), the Wavelet Packet Method (WPM) and the Continuous Wavelet Transform Method (CWT).

## 1.2 Scope and Limitations

The goal of this thesis is to investigate how the accuracy of methods of extracting damping ratios with respect to: three extraction methods, different damping ratios, added noisy data, separated modes and close modes.

To achieve this goal, a simulated analytical signal is analyzed by estimating the modal parameters. The simulated analytic signal is very useful because the exact values are known and the characteristic of the FRF can be varied in order to observe how the accuracy of damping ratios is affected.

The subject of wavelet analysis is a broad and rapidly developing field. There are many different wavelets, but only the Coiflet wavelet and Morlet wavelet are used and evaluated in this study. A survey and evaluation of other wavelets is beyond the scope of the thesis.

## 1.3 Thesis Organization

Chapter 2 gives a brief review of relative theories of the extraction methods.

Principles of WPM and CWT are included.

The implementation of the simulated analytical signal is discussed in Chapter3. The sample rate, number of samples and signal with different damping ratios, noise, separated modes and close modes are defined in detail.

Chapter 4 analyzes the results by comparing those methods. A percent of error is calculated to investigate the accuracy.

A summary of the main points of the thesis and suggestions follow in Chapter5.

The appendix contains theories of CEM and Hilbert transform. The Matlab codes for processing data specified to this thesis are also included.

# Chapter 2

# Theory

## 2.1 The Wavelet Packet Method

### 2.1.1 Wavelet Packet Analysis

The wavelet packet method (WPM) is a generalization of wavelet decomposition that offers a richer signal analysis.

In wavelet analysis, a signal is split into an approximation and a detail. The approximation is then itself split into a second-level approximation and detail, and the process is repeated. For an n-level decomposition, there are n+1 pieces in the decomposition. In wavelet packet analysis, the details as well as the approximations can be split. This yields a decomposition with $2^n$ pieces. Figure 2.1 shows the wavelet packet decomposition tree.

For instance, wavelet packet analysis allows the signal S to be represented as A1 + AAD3 + DAD3 + DD2. This is an example of a representation that is not possible with ordinary wavelet analysis. Wavelet packet nodes are waveforms indexed by three naturally interpreted parameters: position, scale (as in wavelet decomposition), and frequency. For a given orthogonal wavelet function, we generate a library of bases called wavelet packet bases. Each of these bases offers a particular way of coding

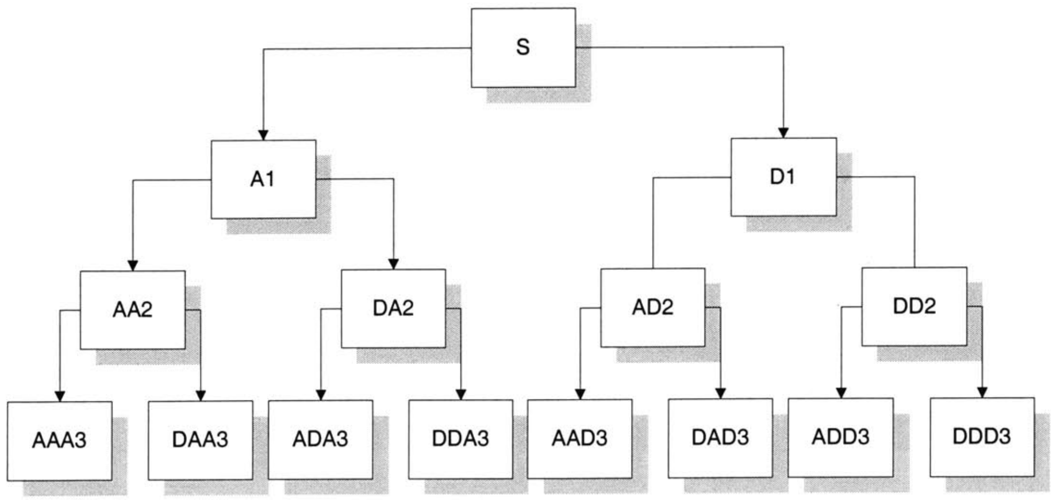


**Figure 2.1** The wavelet packet decomposition tree

signals, preserving global energy and reconstructing exact features. A deep explanation of the wavelet packet analysis can be found in references [8][9][10].

In this project, the Coiflet coif5 wavelet is used.

## 2.1.2 WPM Based Damping Ratio Extraction Procedure

The linear MDOF system is governed by the general equation

$$[M]\ddot{X}+[C]\dot{X}+[K]X = F \tag{2.1}$$

where $[M]$, $[C]$, $[K]$, $F$ are mass, damping, stiffness matrices and excitation vector respectively.

By using modal analysis, $N$ uncoupled equations similar to a SDOF system can be obtained,

$$m_i\ddot{x}_i(t)+c_i\dot{x}_i(t)+k_i x_i(t)= f_i(t), \tag{2.2}$$

for $i = 1,2,\dots,N$. The impulse response of this MDOF system can be given in general form as

$$. \; h(t)=\sum_{i=1}^{N} A_i e^{-\zeta_i w_{n_i} t}\sin\left(\sqrt{1-\zeta_i^2}\, w_{n_i} t+\psi_i\right) \tag{2.3}$$

where $w_{n_i}$ is the natural frequency, $N$ is the number of modes considered, $A_i$ is the residue magnitude of the $i$ th mode and $\zeta_i$ is the damping ratio. This response represents a linear combination of its signal modal components. Each mode is given by an exponentially decaying harmonic function.

As discussed in section 2.1.1, the signal, an impulse response of a MDOF system, can be split into wavelet packet nodes. Each node represents a filtered range of frequencies. By analyzing the FRF of each node, a certain number of nodes is assigned to each mode, which has the frequency response most similar to those of the assigned nodes. After reconstructing the IRF of each mode, damping ratios can then be extracted using the Hilbert transform as shown in Appendix B. The WPM based procedure above is shown schematically in Figure 2.2.

## 2.2 The Continuous Wavelet Transform

### 2.2.1 The Morlet Wavelet

In the early 1980s, Morlet introduced a ‘wavelet', which was dilated and translated to form a family of analyzing functions. These functions are given by

$$\psi_{a,b}(t) = \frac{1}{\sqrt{a}}\psi(\frac{t-b}{a}) \tag{2.4}$$

which is a dilation (denoted by a) and translation (denoted by b) of the mother wavelet $\psi(t)$. The continuous wavelet transform (CWT) is defined as

$$W(a,b) = \int f(t)\overline{\psi_{a,b}(t)}dt \tag{2.5}$$

where the bar denotes complex conjugation. The wavelet transform computes the correlation between the signal and the dilation and translation of the wavelet $\psi(t)$. The coefficients are therefore a measure of the similarity between the wavelet and the function $f(t)$ [8][9][11].

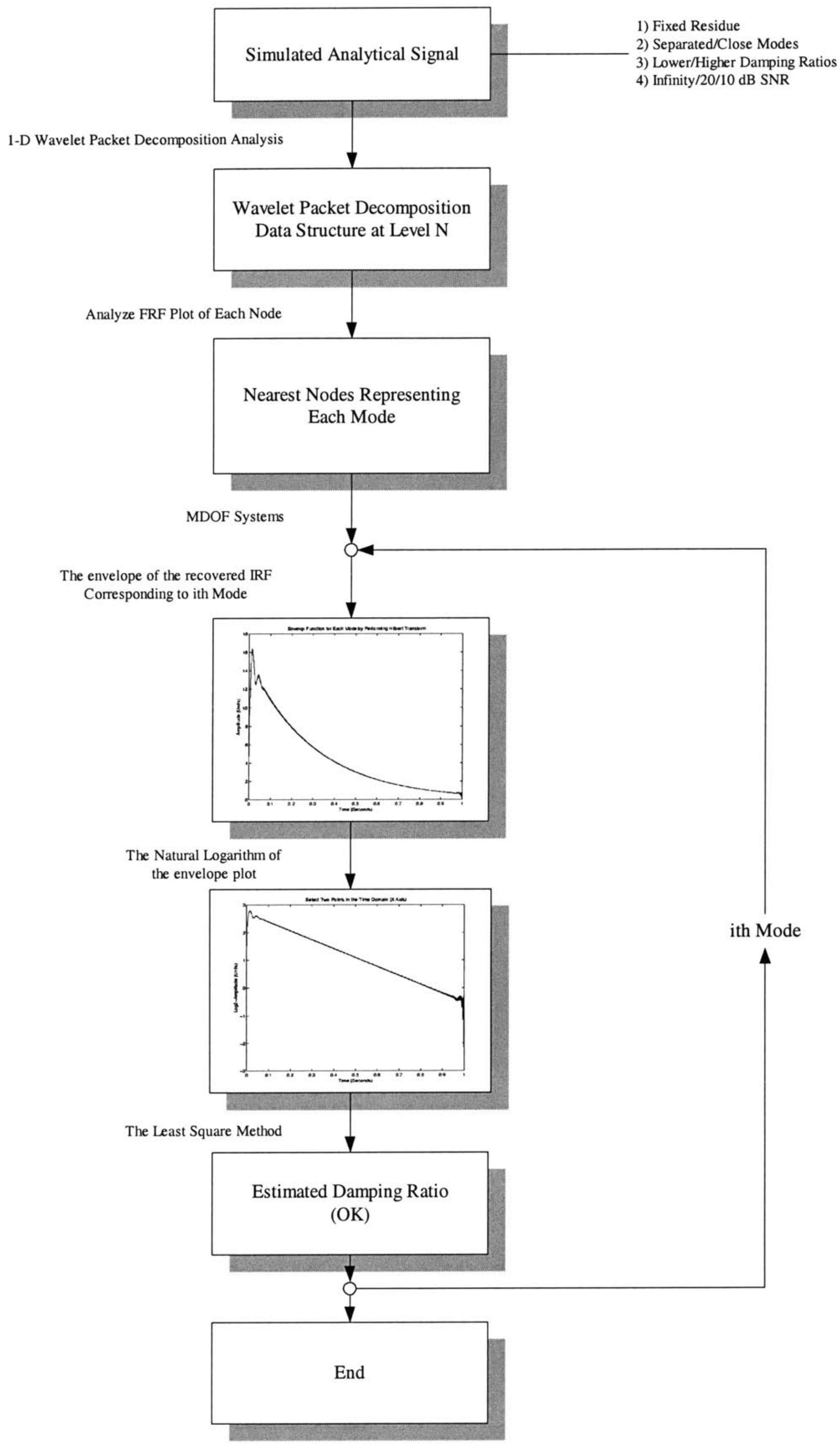


**Figure 2.2** The WPM based damping ratio extraction procedure

The Morlet wavelet used in this project is defined as

$$\psi_M(t) = e^{iw_0 t} e^{-\left(\frac{t}{\alpha}\right)^2} \tag{2.6}$$

Traditionally, the parameters $\alpha$ and $w_0$ are defined as

$$\alpha = \sqrt{2}$$
$$w_0 = \pi\sqrt{\frac{2}{\ln 2}} \tag{2.7}$$

The Fourier spectrum of the Morlet wavelet is a shifted Gaussian function [6]

$$G(f) = \sqrt{2\pi} e^{-2\pi^2\left(f - {w_0}/{2\pi}\right)^2} \tag{2.8}$$

The corresponding wavelet is plotted in Figure 2.3.

## 2.2.2 CWT Based Damping Ratio Extraction Procedure

For a SDOF system given by equation (2.2), when the damping term $(c/2m)^2 << 1$, the solution of the system can be given in the form of an analytic signal

$$x(t) = A(t)e^{\pm i w_n \sqrt{1-\zeta^2} t} = A(t)e^{i\phi(t)} \tag{2.9}$$

Assuming that the envelope $A(t)$ is slowly varying, the Morlet wavelet transform of the equation (2.9) can be approximated as [6][12]

$$(w_g x)(a,b) \approx A(b) G^*\left(\left(a\dot{\phi}(b)\right)\right) e^{i\phi(b)} + O\left(\left|\dot{A}\right|, \left|\ddot{\phi}\right|\right) \tag{2.10}$$

where $G^*(\cdot)$ denotes the complex conjugate of $G(\cdot)$. The modulus of this function is given by

$$\left|(w_g x)(a,b)\right| \approx A(b)\left|G^*\left(a\dot{\phi}(b)\right)\right| \tag{2.11}$$

For a given value of dilation, $a_0$, equation (2.11) can be rewritten as

$$\left|(w_g x)(a_0,b)\right| \approx A_0 e^{-\zeta w_n b}\left|G^*\left(\pm i a_0 w_n \sqrt{1-\zeta^2}\right)\right| \tag{2.12}$$

Taking the natural logarithm of each side yields,

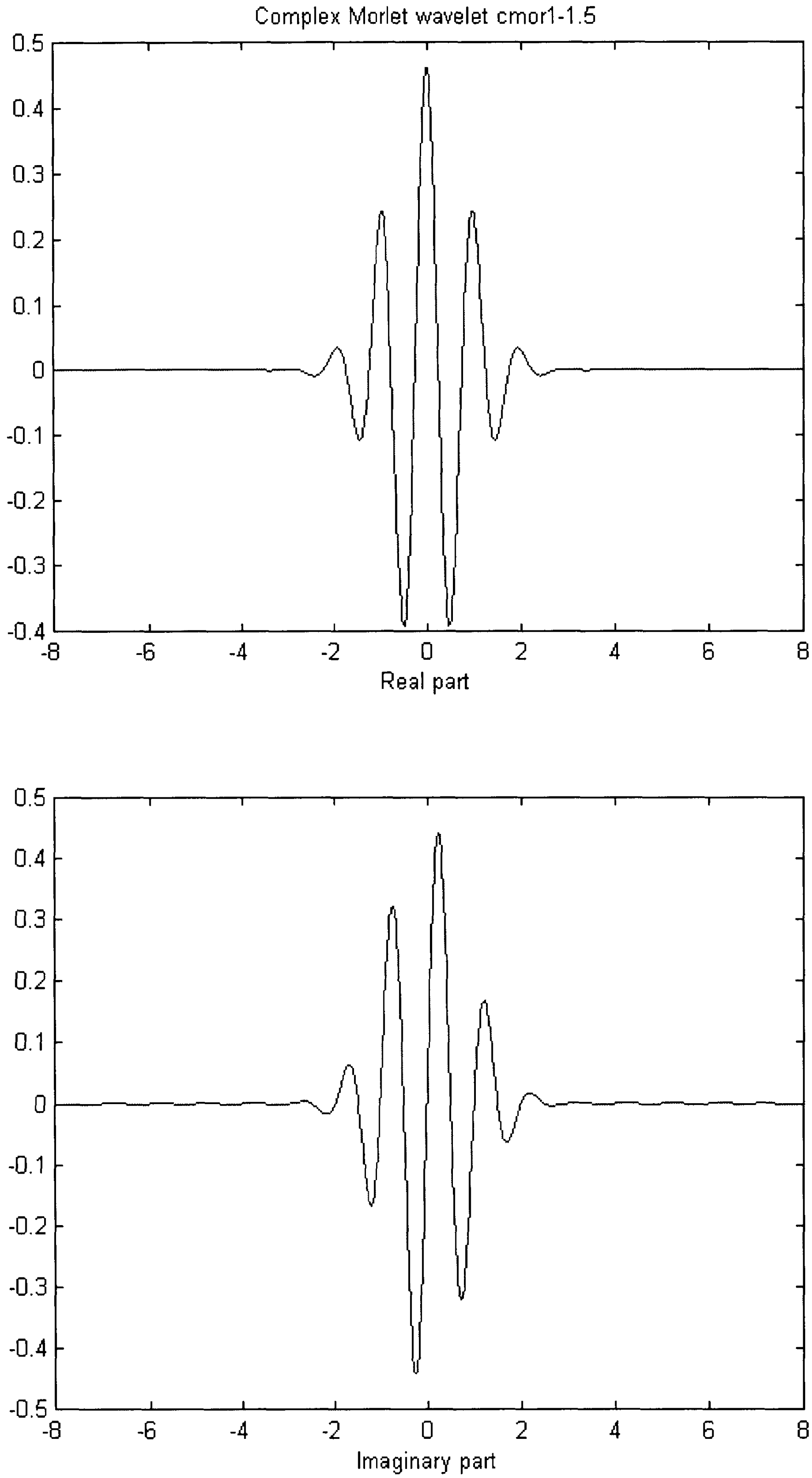


**Figure 2.3** The complex Morlet wavelet: cmor

$$\ln\left|\left(w_g x\right)\left(a_0, b\right)\right| \approx -\zeta w_n b + \ln\left( A_0 \left| G^*\left(\pm i a_0 w_n \sqrt{1-\zeta^2}\right)\right|\right) \tag{2.13}$$

Thus the damping ratio $\zeta$ of the system can be estimated from the slope of the straight line of the wavelet modulus $\left|\left(w_g x\right)\left(a_0, b\right)\right|$ plotted in a natural logarithm scale.

The procedure can be extended to a MDOF system on the assumption that the MDOF system governed by equation (2.1) can be uncoupled. Equation (2.12) and (2.13) can then be rebuilt for a MDOF system as

$$\left|\left(w_g x_i\right)\left(a_i, b\right)\right| \approx A_i e^{-\zeta_i w_{n_i} b} \left| G^*\left(\pm i a_i w_{n_i} \sqrt{1-\zeta^2}\right)\right| \tag{2.14}$$

$$\ln\left|\left(w_g x_i\right)\left(a_i, b\right)\right| \approx -\zeta_i w_{n_i} b + \ln\left( A_i \left| G^*\left(\pm i a_i w_{n_i} \sqrt{1-\zeta_i^2}\right)\right|\right) \tag{2.15}$$

for $i = 1, 2, \ldots, N$.

The damping ratio $\zeta_i$ of the $i$th mode can be estimated from equation (2.15) as the slope of the straight line of the wavelet modulus $\left|\left(w_g x_i\right)\left(a_i, b\right)\right|$, for the given values of dilation $a_i$ related to the natural frequency $f_{n_i}$ of the system, plotted against b in a natural logarithm scale [6][12]. The CWT based procedure above is shown schematically in Figure 2.4.

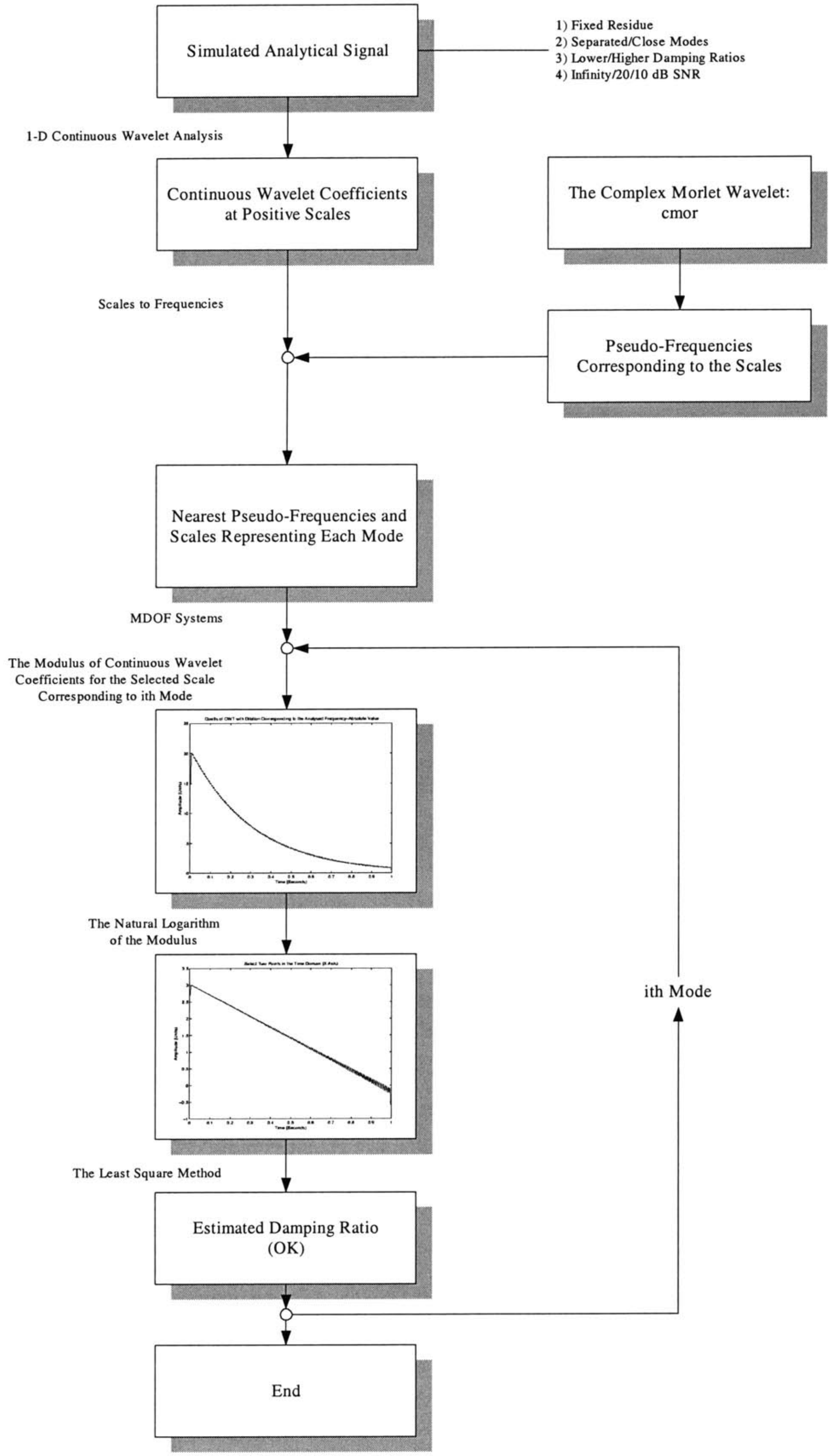


**Figure 2.4** The CWT based damping ratio extraction procedure

# Chapter 3

# Implementation Procedure

## 3.1 General Procedure

In order to evaluate the accuracy of extracting damping ratios by the three methods proposed in the previous chapter, several simulations are performed. The simulated analytic signal is set with known properties. The algorithms based on the methods of CEM, WPM, CWT are coded in Matlab 6.0 written specifically for this thesis. The details of this implementation can be found in Appendix C.

For simplicity, the impulse response of the 3-DOF systems is simulated. However, it is assumed that the procedure can be extended to general MDOF systems. By setting the damping ratio of the first mode and adding specified noise, a simulated signal can be generated. Three extraction methods are then provided to perform the estimation. Different input parameters are required for each method. The main menu for choosing one of three methods is shown in Figure 3.1.

## 3.2 Simulated Analytical Signal

### 3.2.1 Signal Parameters

In this section the parameters of the simulated analytical data sets are presented.

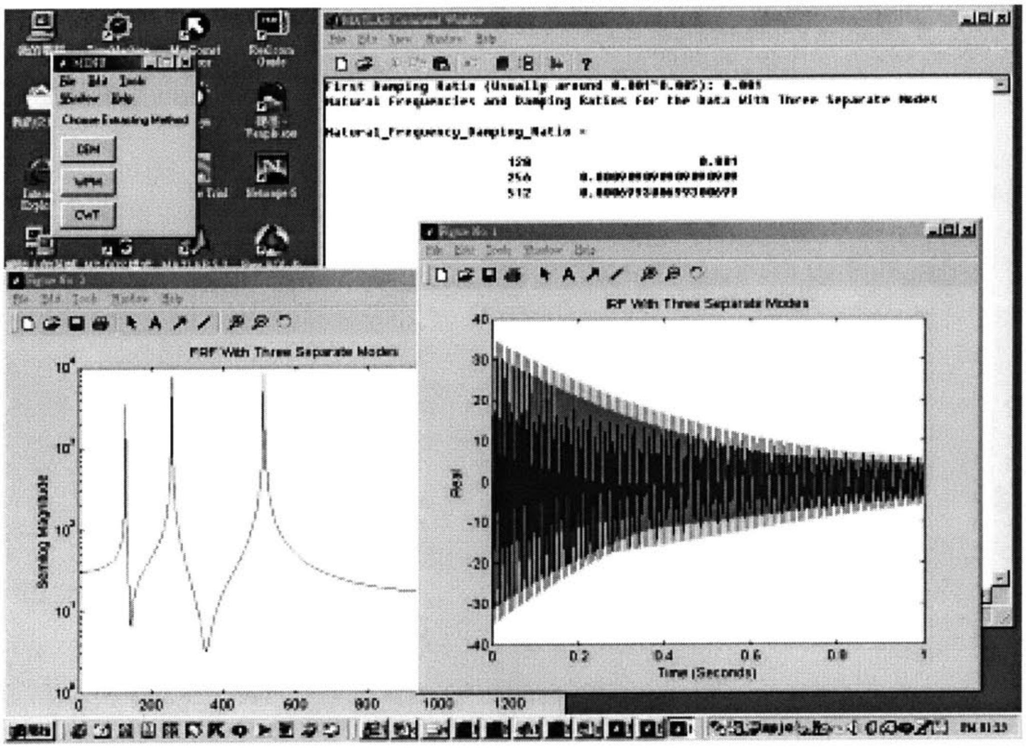


**Figure 3.1** The user interface of three methods for extracting damping ratios

Table 3.1 gives the sampling parameters in the signal.

**Table 3.1** Sampling parameters in the signal

| Sample Rate | Number of Samples |
|---|---|
| 2048 Hz | 2048 |

The accuracy of three methods with respect to signals having separated modes and close modes, different damping ratios and noisy data, is discussed. In this thesis, only the underdamped case, which is $0 < \zeta < 1$, is considered and is the one usually encountered. The underdamped system oscillates with a decaying amplitude and a frequency $w_n(1-\zeta^2)^{1/2}$, somewhat less than the frequency of the undamped oscillation. Values of 0.001 and 0.02 are used for lower and higher damping ratios of the first mode respectively. Damping ratios are assumed to increase linearly with the modal frequencies [1]. The properties of simulated analytical data sets with separated and close modes are presented in Table 3.2 and 3.3 respectively. The IRF, FRF plots for each simulated data set are represented in Figure 3.2 and 3.3. The properties of simulated analytical data set with higher damping ratios are presented in Table 3.4. The IRF, FRF plots are represented in Figure 3.4.

**Table 3.2** Properties of the simulated data set with separated modes and lower damping ratios

| Mode | Residue | Natural Frequency | Damping Ratio |
|---|---|---|---|
| 1 | 5 | 128 | 0.0010000000 |
| 2 | 15 | 256 | 0.0020000000 |
| 3 | 22.5 | 512 | 0.0040000000 |

**Table 3.3** Properties of the simulated data set with close modes

| Mode | Residue | Natural Frequency | Damping Ratio |
|---|---|---|---|
| 1 | 5 | 256 | 0.0010000000 |
| 2 | 15 | 307.2 | 0.0012000000 |
| 3 | 22.5 | 399.36 | 0.0015600000 |

**Table 3.4** Properties of the simulated data set with separated modes and higher damping ratios

| Mode | Residue | Natural Frequency | Damping Ratio |
|---|---|---|---|
| 1 | 5 | 128 | 0.0200000000 |
| 2 | 15 | 256 | 0.0400000000 |
| 3 | 22.5 | 512 | 0.0800000000 |

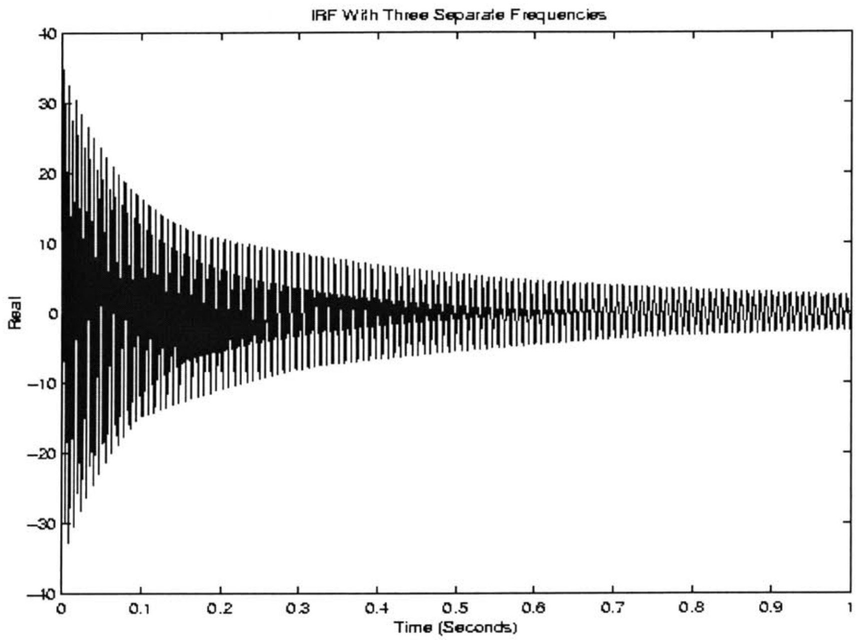


(a) IRF plot

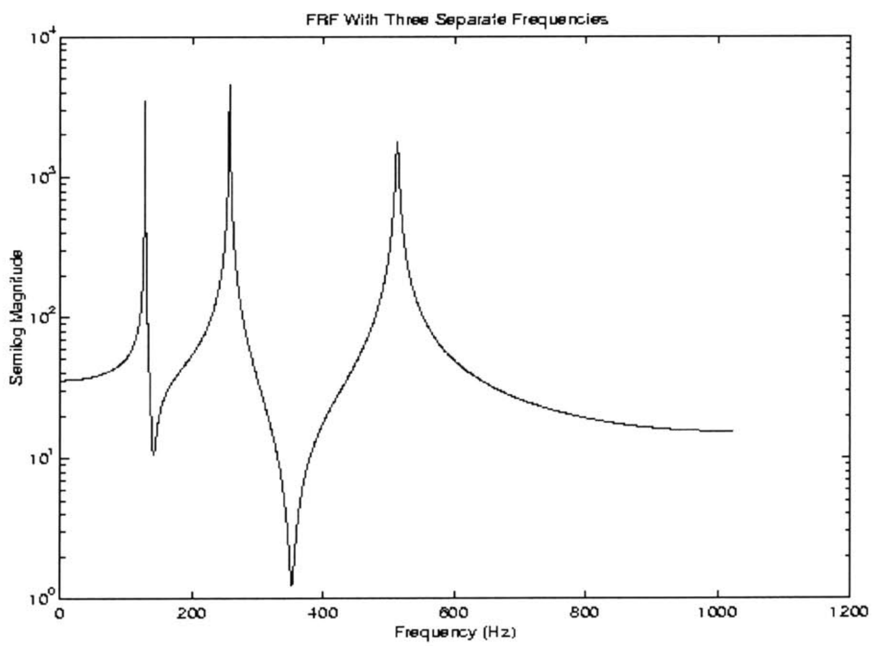


(b) FRF plot

**Figure 3.2** (a) IRF and (b) FRF plot of the simulated data set with separated modes, lower damping ratios and no noise (SNR = $\infty$ dB)

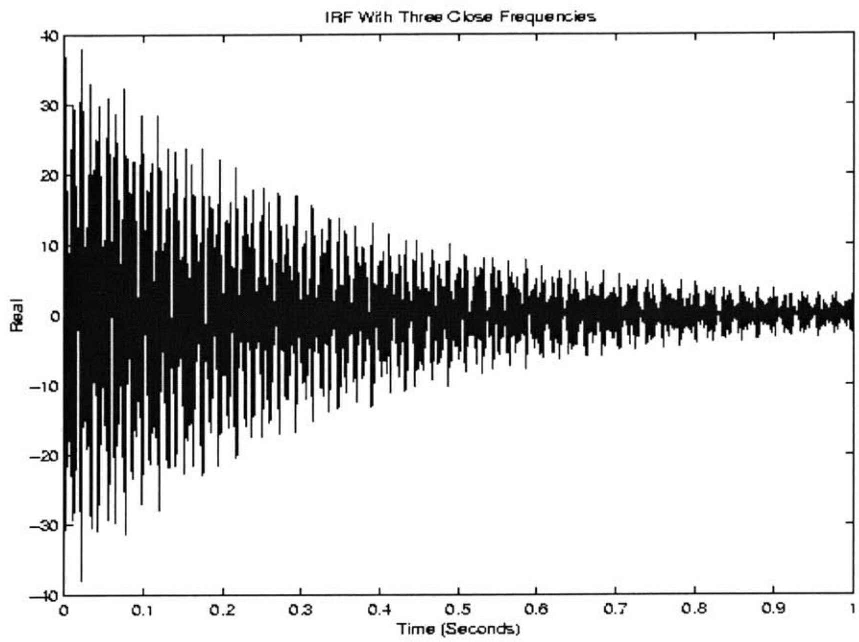


(a) IRF plot

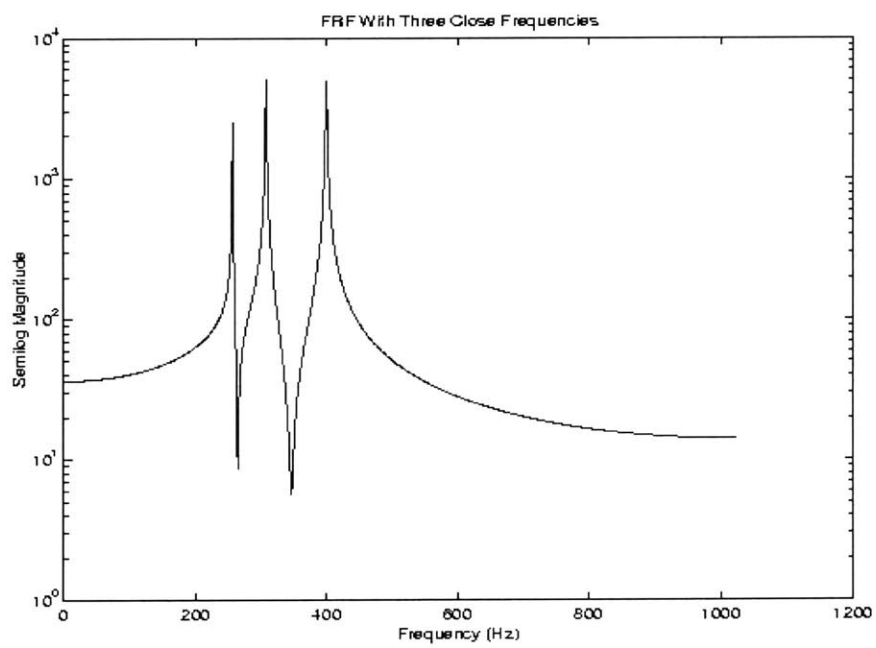


(b) FRF plot

**Figure 3.3** (a) IRF and (b) FRF plot of the simulated data set with close modes and no noise (SNR = $\infty$ dB)

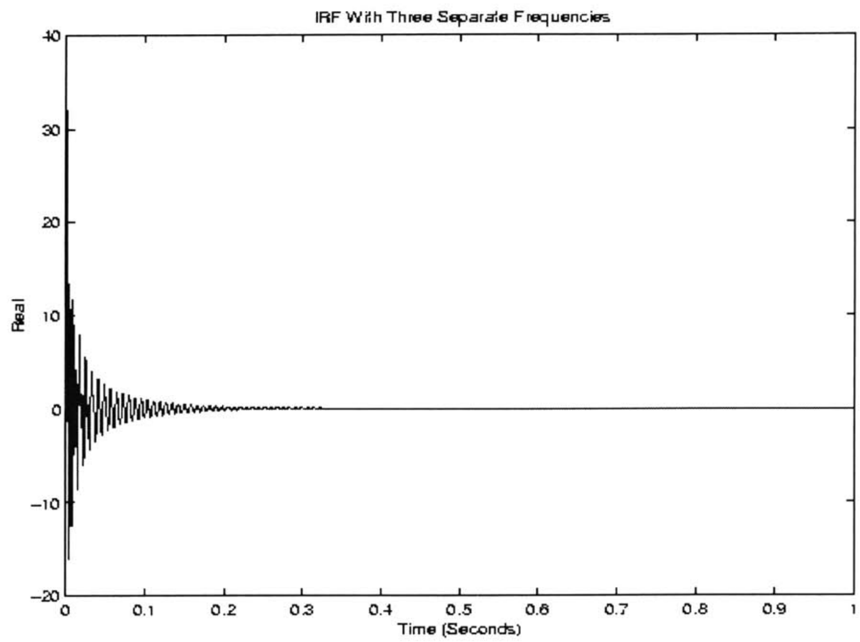


(a) IRF plot

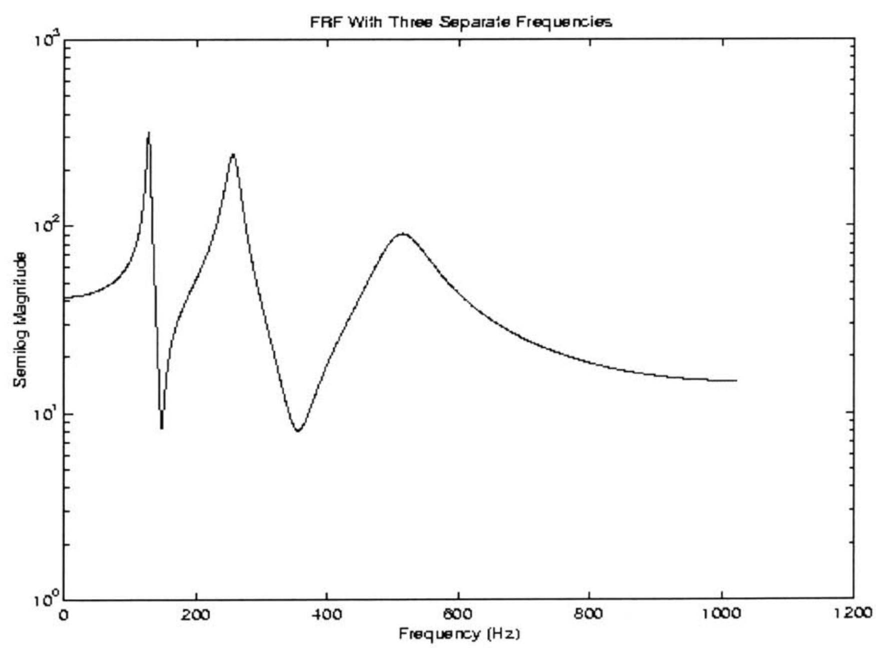


(b) FRF plot

**Figure 3.4** (a) IRF and (b) FRF plot of the simulated data set with separated modes, higher damping ratios and no noise (SNR = $\infty$ dB)

The simulated signal is also corrupted by zero mean Gaussian noise, as discussed in the next section.

### 3.2.2 Signal-to-Noise Ratio

In analog and digital communications, signal-to-noise ratio, SNR, is a measure of signal strength relative to background noise. The ratio is usually measured in decibels (dB). The formula is given by

$$SNR = 10\log_{10}\left(\frac{\sigma_s^2}{\sigma_n^2}\right) \tag{3.1}$$

where $\sigma_s^2$ is the signal variance and $\sigma_n^2$ is the noise variance.

Given a signal, $s(t)$ with known $\sigma_s$, and desired SNR, the generated noise signal is

$$n(t) = \sigma_n N(0,1) \tag{3.2}$$

where $N(0,1)$ is a Normally (Gaussian) distributed random variable with zero mean and unit variance.

In the simulation, SNR is set equal to $\infty$ dB, 20 dB and 10 dB. Figure 3.5 shows the IRF and FRF of the simulated data set with separated modes, lower damping ratios and noisy data (SNR = 20 dB)

### 3.2.3 Error Measurement

In order to evaluate the damping ratio accuracy, a percentage error defined in equation (3.3) is calculated.

$$Err(\%) = \frac{\zeta_e - \zeta_t}{\zeta_t} \times 100\% \tag{3.3}$$

where $\zeta_e$ is the estimated damping ratio and $\zeta_t$ is the theoretical damping ratio.

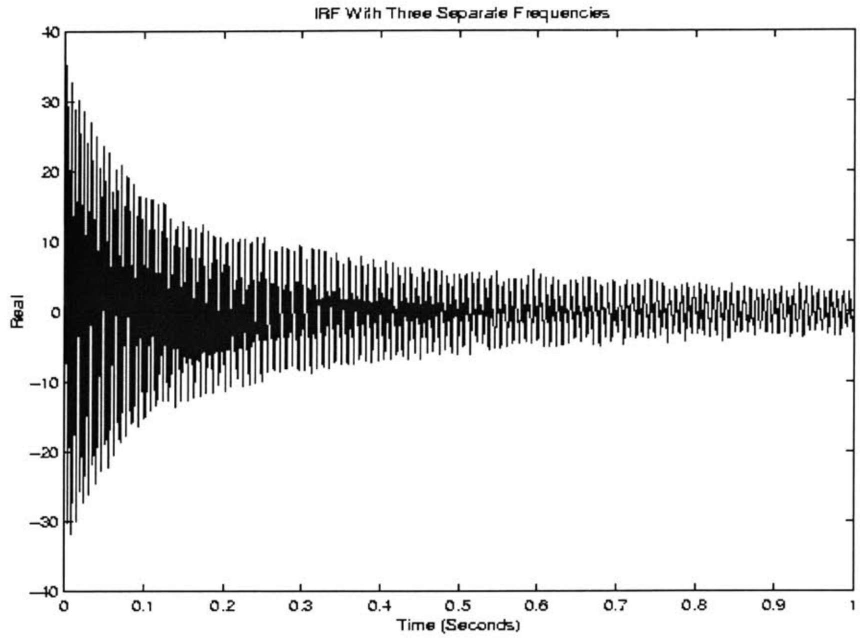


(a) IRF plot

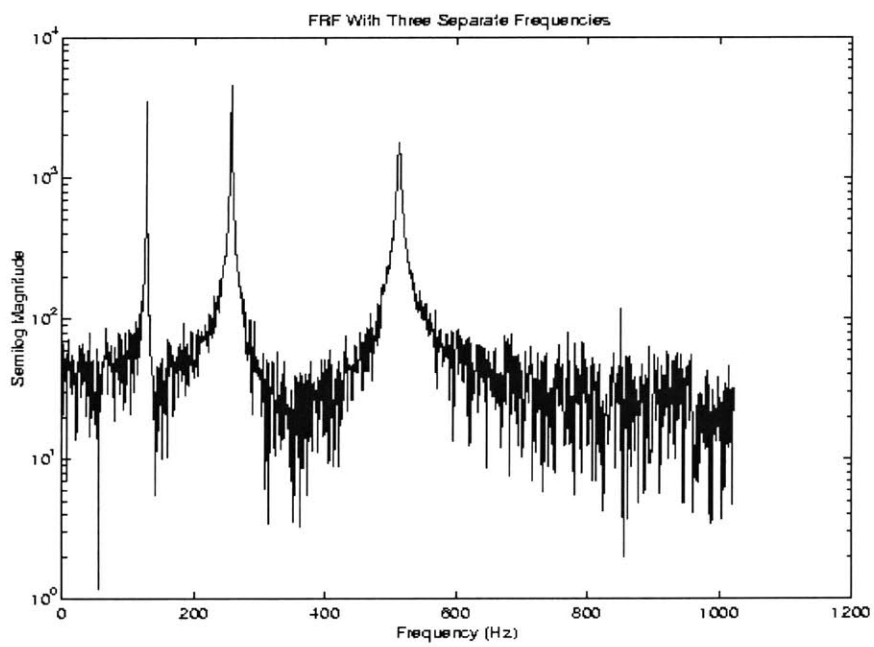


(b) FRF plot

**Figure 3.5** (a) IRF and (b) FRF plot of the simulated data set with separated modes, lower damping ratios and noisy data (SNR = 20 dB)

# Chapter 4

# Results and Discussion

## 4.1 Simulated Analytical Signal With Separated Modes

This part summarizes the results of the three methods for extracting damping ratios, for the separated modes. The frequencies corresponding to the separated modes are 128, 256, 512 (Hz). Other parameters of the signal are defined in Chapter 3.

### 4.1.1 CEM Results

This method requires two additional input parameters: DOF and truncation of frequencies to perform. The effect of truncation becomes important if the truncation limits are close to the modal frequencies. The problem with the truncation is that when the IRF is calculated it has time leakage and some information is lost, therefore the estimated damping ratio will deviate from the exact solution. Table 4.1 represents an example with truncation limits between 58.06 and 611.10 (Hz). A complete development of this method is shown in Appendix A.

In order to avoid the effect of truncation, only cases without truncation are considered, i.e. the entire range of frequency from 0 to 1024 (Hz) is taken to process. Figure 4.1 shows IRF, FRF and phase angle plot of the simulated and fitted curve with lower

**Table 4.1** Estimation results with truncation for separated modes

| Frequency (Hz) | Theoretical Value ($\zeta_t$) | SNR (dB) | Estimated Value ($\zeta_e$) | Error (%) |
|---|---|---|---|---|
| 128 | 0.0010000000 | $\infty$ | 0.2365217096 | 23552.2 |
| 256 | 0.0020000000 | $\infty$ | 0.0176099322 | 780.5 |
| 512 | 0.0040000000 | $\infty$ | 0.0032943060 | -17.6 |

damping ratios and noisy data (SNR = 20 dB). Table 4.2 and 4.3 summarize the results without truncation.

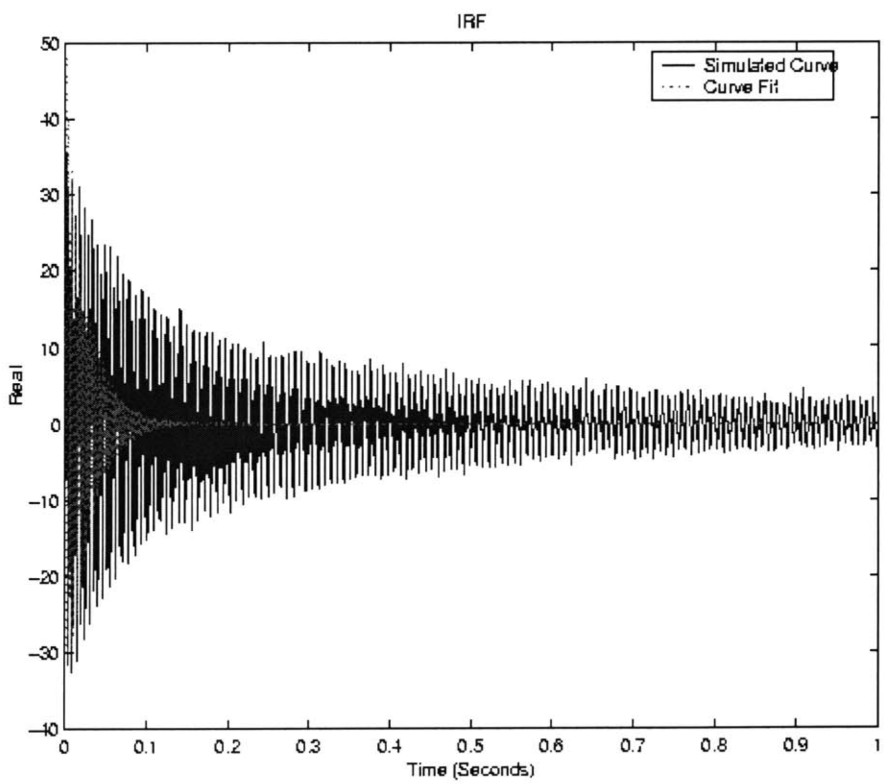


(a) IRF plot of the simulated and fitted curve

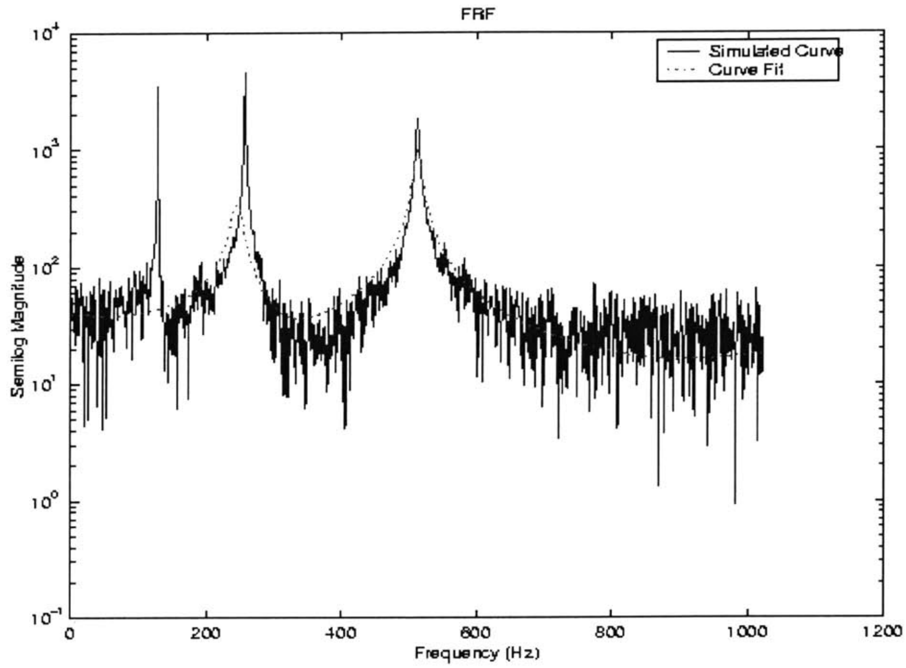


(b) FRF plot of the simulated and fitted curve

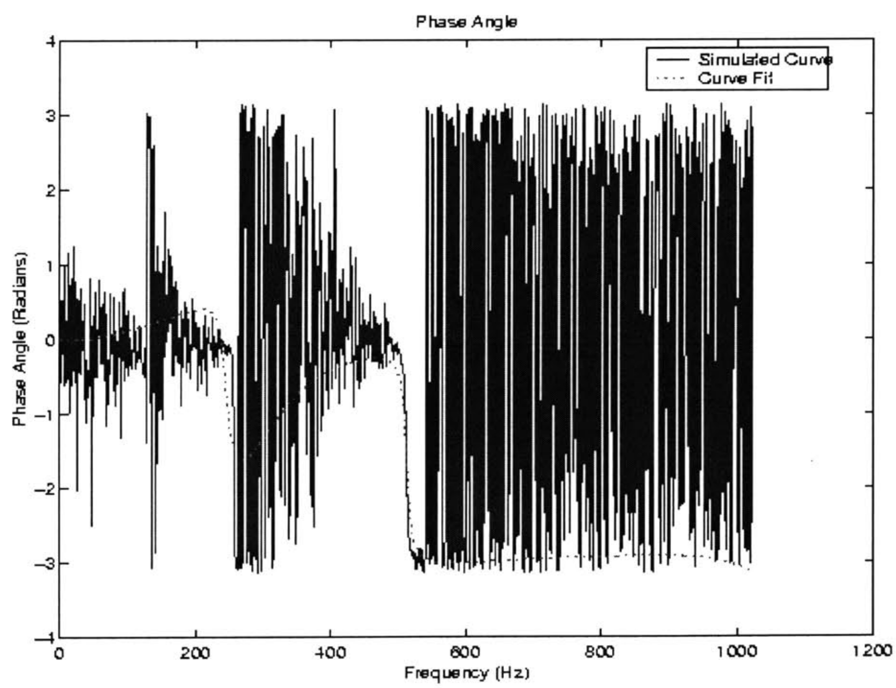


(c) Phase angle plot of the simulated and fitted curve

**Figure 4.1** (a) IRF, (b) FRF and (c) phase angle plot of the simulated and fitted curve with separated modes, lower damping ratios and noisy data (SNR = 20 dB)

**Table 4.2** Estimation results based on the CEM with lower damping ratios for separated modes

| Frequency (Hz) | Theoretical Value ($\zeta_t$) | SNR (dB) | Estimated Value ($\zeta_e$) | Error (%) |
|---|---|---|---|---|
| 128 | 0.0010000000 | ∞ | 0.0010000002 | 0.0 |
| | | 20 | 0.0800783134 | 7907.8 |
| | | 10 | 0.0791687633 | 7816.9 |
| 256 | 0.0020000000 | ∞ | 0.0020000000 | 0.0 |
| | | 20 | 0.0335427316 | 1577.1 |
| | | 10 | 0.1075900155 | 5279.5 |
| 512 | 0.0040000000 | ∞ | 0.0039999998 | 0.0 |
| | | 20 | 0.0106645845 | 166.6 |
| | | 10 | 0.0428453288 | 971.1 |

**Table 4.3** Estimation results based on the CEM with higher damping ratios for separated modes

| Frequency (Hz) | Theoretical Value ($\zeta_t$) | SNR (dB) | Estimated Value ($\zeta_e$) | Error (%) |
|---|---|---|---|---|
| 128 | 0.0200000000 | ∞ | 0.0200000029 | 0.0 |
| | | 20 | 0.1056261912 | 428.1 |
| | | 10 | 0.0676097338 | 238.0 |
| 256 | 0.0400000000 | ∞ | 0.0400000039 | 0.0 |
| | | 20 | 0.0911037669 | 127.8 |
| | | 10 | 0.1697063481 | 324.3 |
| 512 | 0.0800000000 | ∞ | 0.0799999978 | 0.0 |
| | | 20 | 0.0908770838 | 13.6 |
| | | 10 | 0.1300957561 | 62.6 |

### 4.1.2 WPM Results

In this method, we first generate a library of wavelet packet bases for a given orthogonal wavelet function, coif5. The decomposition level is set at 5 therefore $2^5 = 32$ sets of coefficients are generated. By reconstructing the coefficients and visualizing the FRF of each recovered IRF, we can select the most suitable nodes, which are numbered from AAAAA5 to DDDDD5 as Node1 to Node32 at level 5, to represent a specified mode. The FRF of selected nodes are shown in Figure 4.2, 4.3 and 4.4. The response of each mode is then the summation of the selected nodes. In order to find the envelope of each response, the Hilbert transform is performed. After taking the natural logarithm of the envelope plot, a linear plot is obtained. The results are shown in Figure 4.5, 4.6 and 4.7. The Least Square Method is then applied to find the regression line. The damping ratio can be calculated from the slope of the regression line. Table 4.4 summarizes the selected nodes corresponding to three modes.

**Table 4.4** Summary of selected nodes corresponding to three separated modes

| Frequency (Hz) | Selected Nodes |
|---|---|
| 128 | Node(3), Node(7) |
| 256 | Node(5), Node(13) |
| 512 | Node(9), Node(25) |

Table 4.5 and 4.6 summarize the estimation results with lower damping ratios and higher damping ratios respectively. Figure 4.8 shows the IRF and FRF of the simulated and fitted curve, which is obtained by adding the effects of the selected six nodes, with lower damping ratios and no noise added.

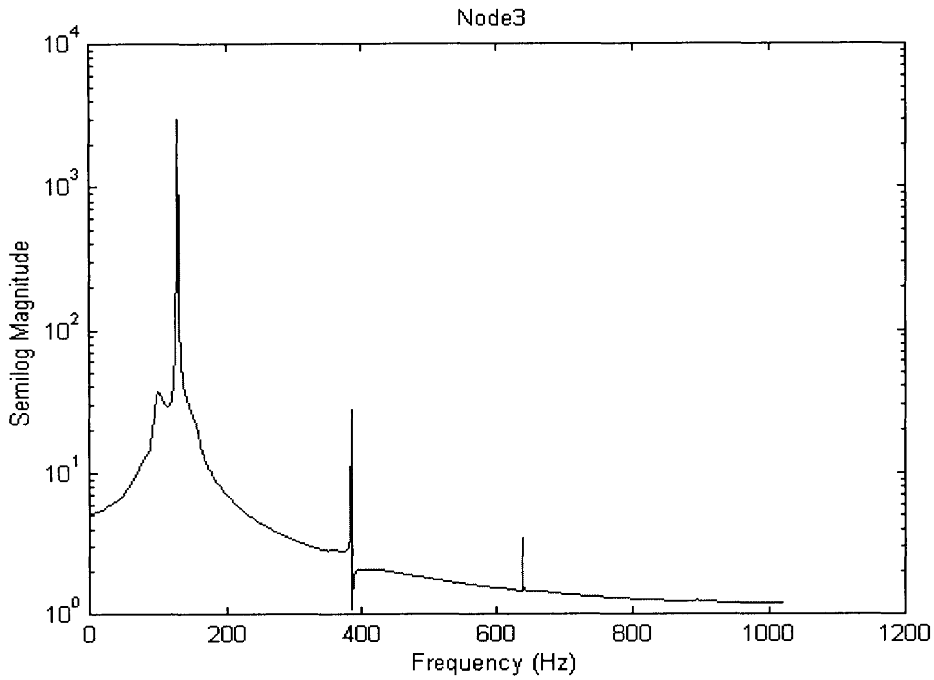


(a) FRF plot of wavelet packet node 3

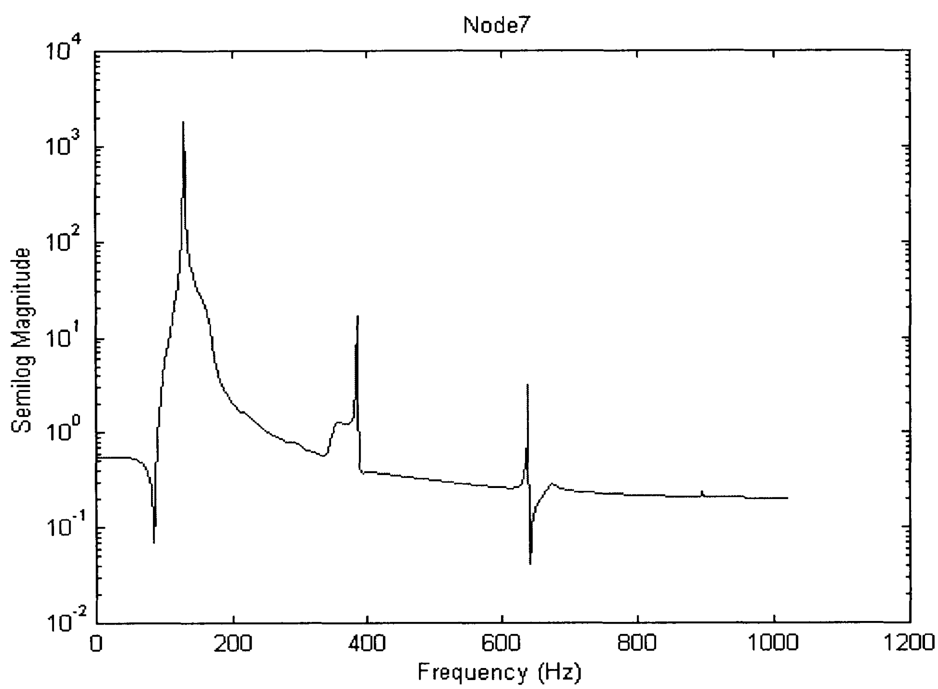


(b) FRF plot of wavelet packet node 7

**Figure 4.2** (a) FRF plot of wavelet packet node 3 and (b) node 7 representing the first mode (128 Hz) with lower damping ratios and no noise (SNR = $\infty$ dB)

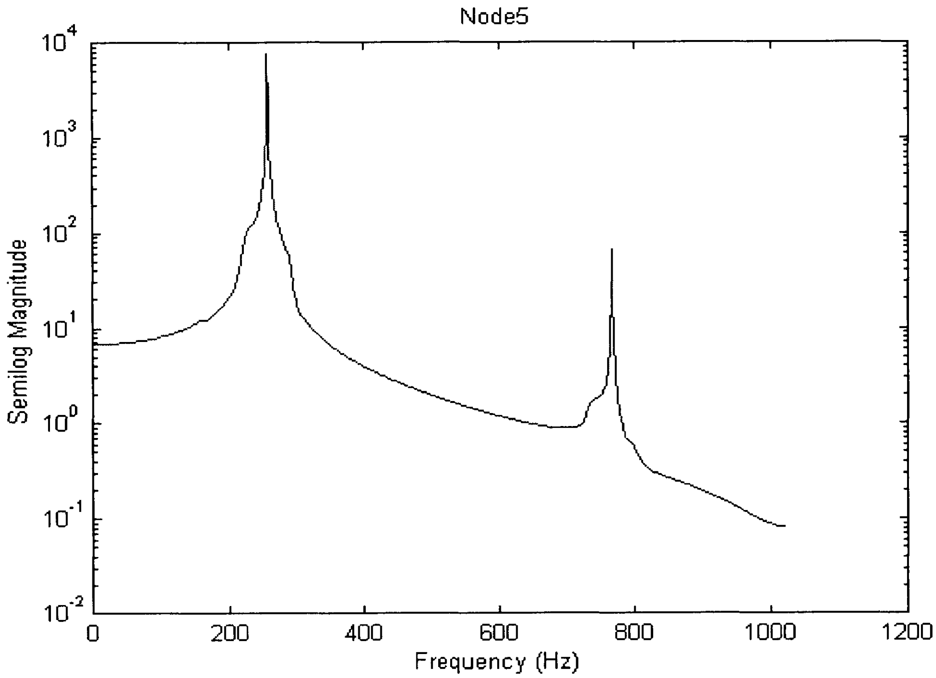


(a) FRF plot of wavelet packet node 5

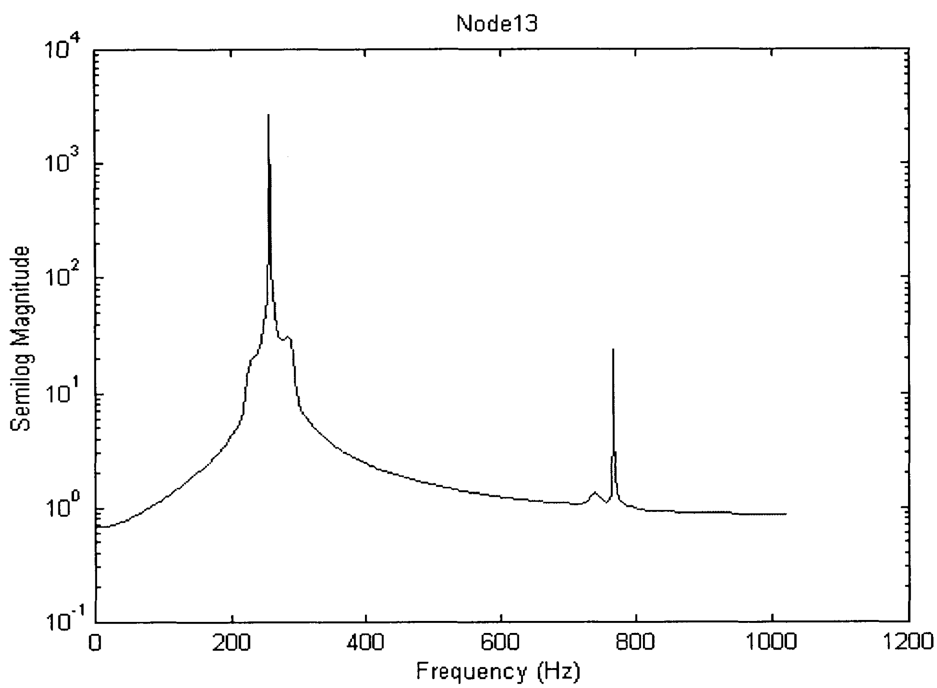


(b) FRF plot of wavelet packet node 13

**Figure 4.3** (a) FRF plot of wavelet packet node 5 and (b) node 13 representing the second mode (256 Hz) with lower damping ratios and no noise (SNR = $\infty$ dB)

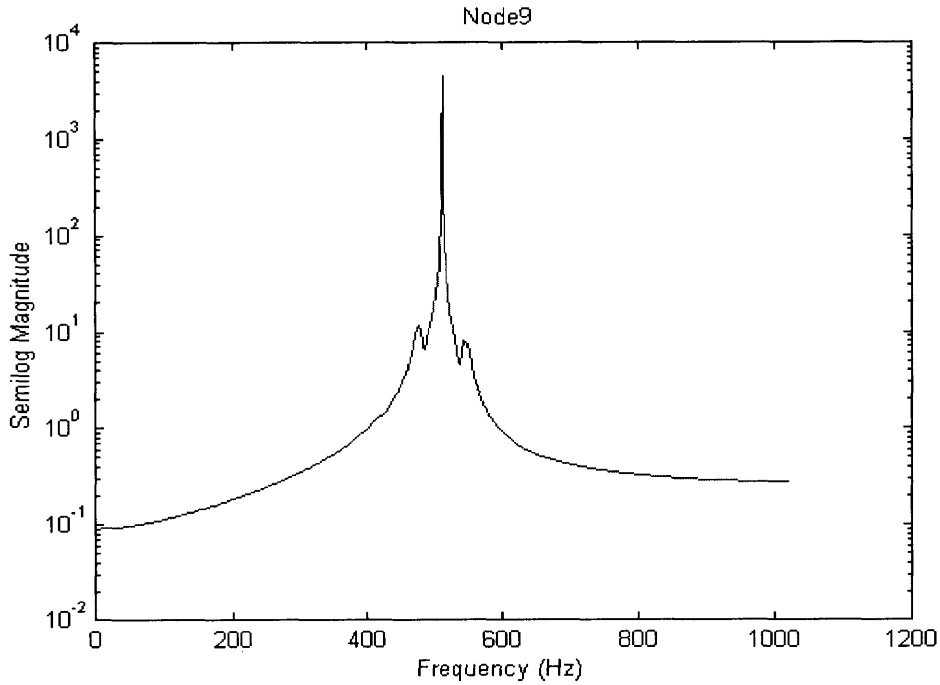


(a) FRF plot of wavelet packet node 9

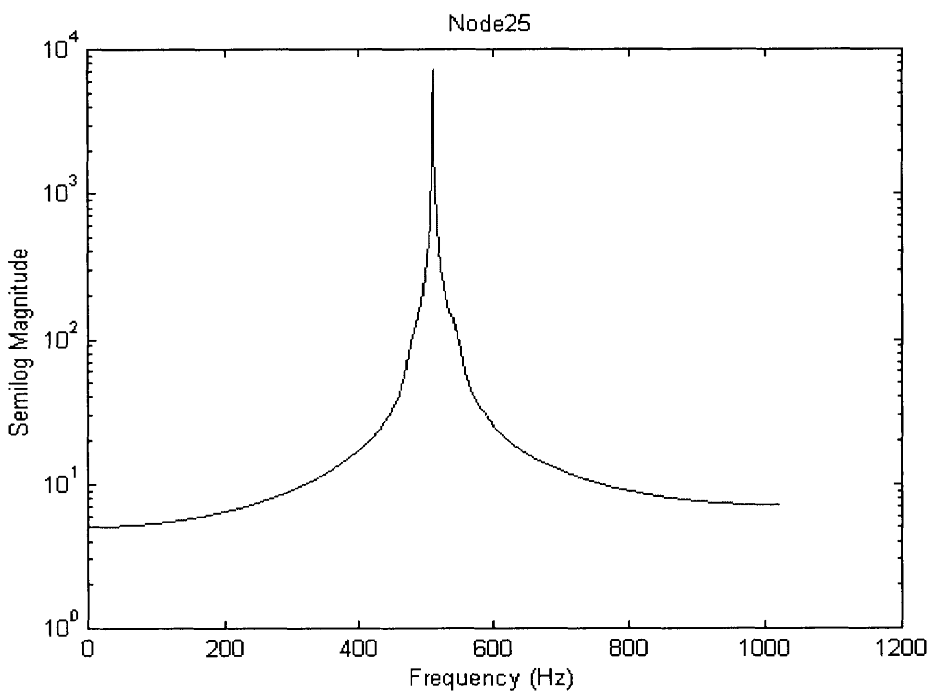


(b) FRF plot of wavelet packet node 25

**Figure 4.4** (a) FRF plot of wavelet packet node 9 and (b) node 25 representing the third mode (512 Hz) with lower damping ratios and no noise (SNR = $\infty$ dB)

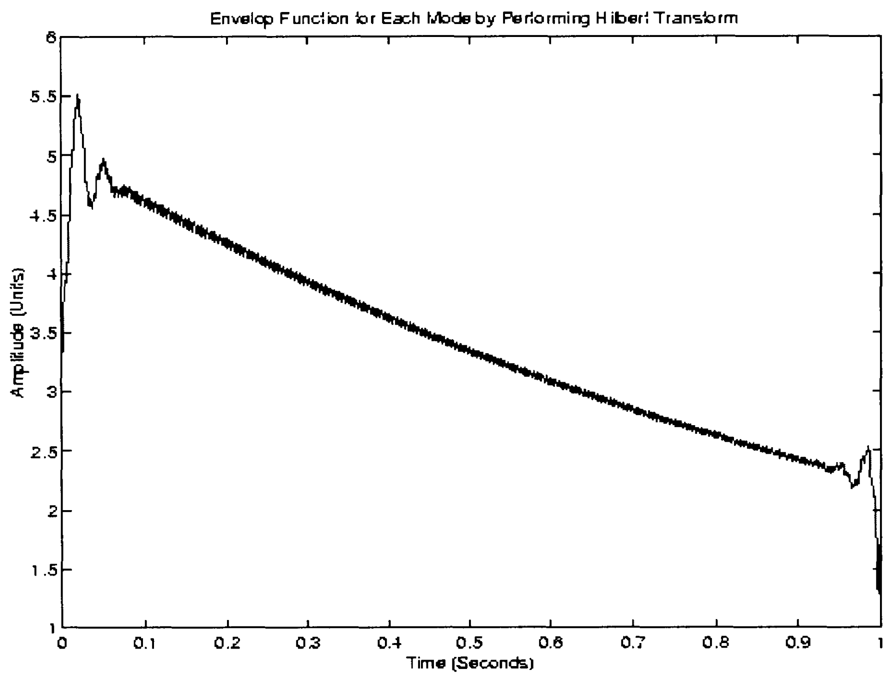


(a) The envelope plot of the recovered IRF

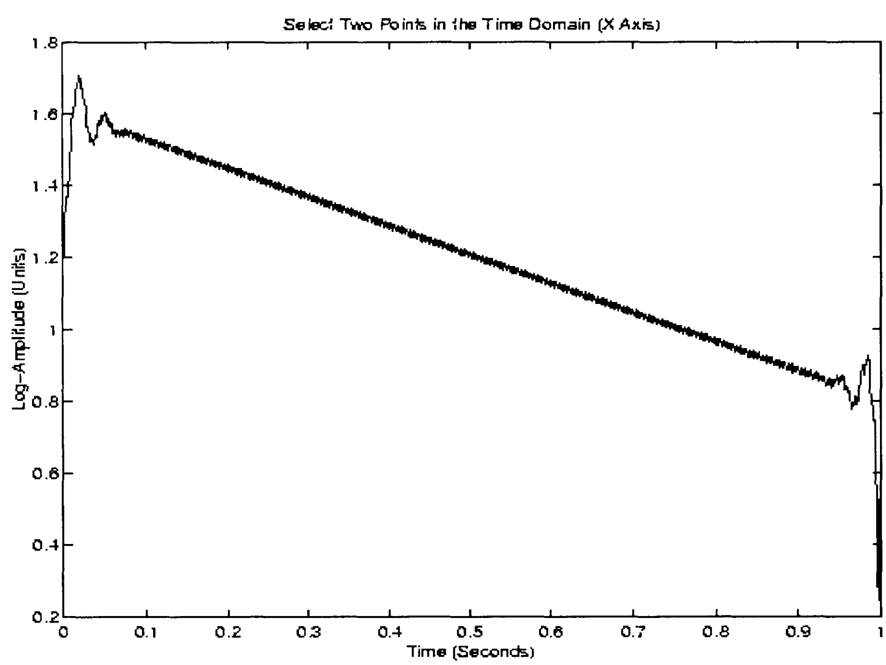


(b) The natural logarithm of the envelope plot

**Figure 4.5** (a) The envelope plot of IRF and (b) the natural logarithm of the envelope plot for the first mode (128 Hz) with lower damping ratios and no noise (SNR = $\infty$ dB)

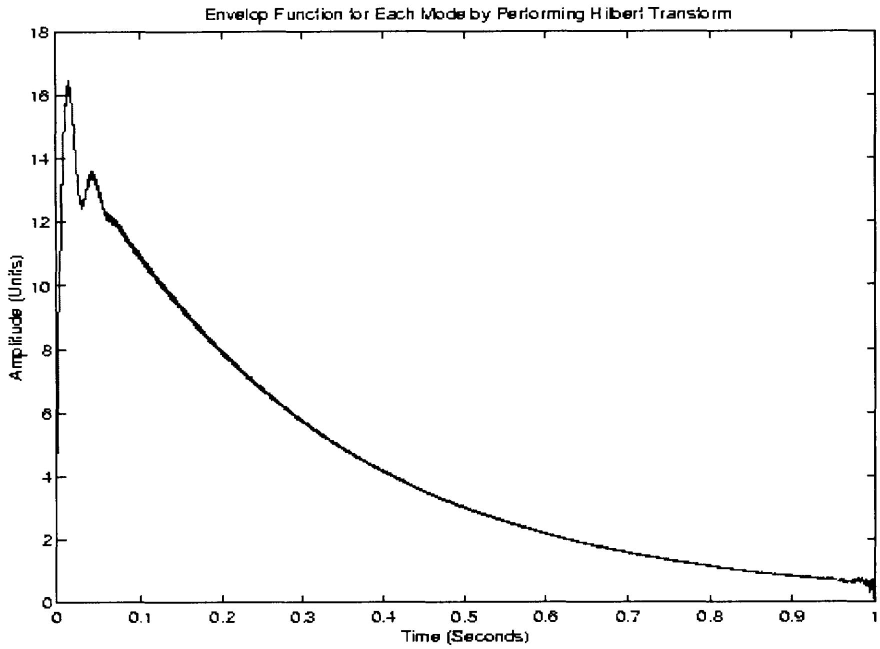


(a) The envelope plot of the recovered IRF

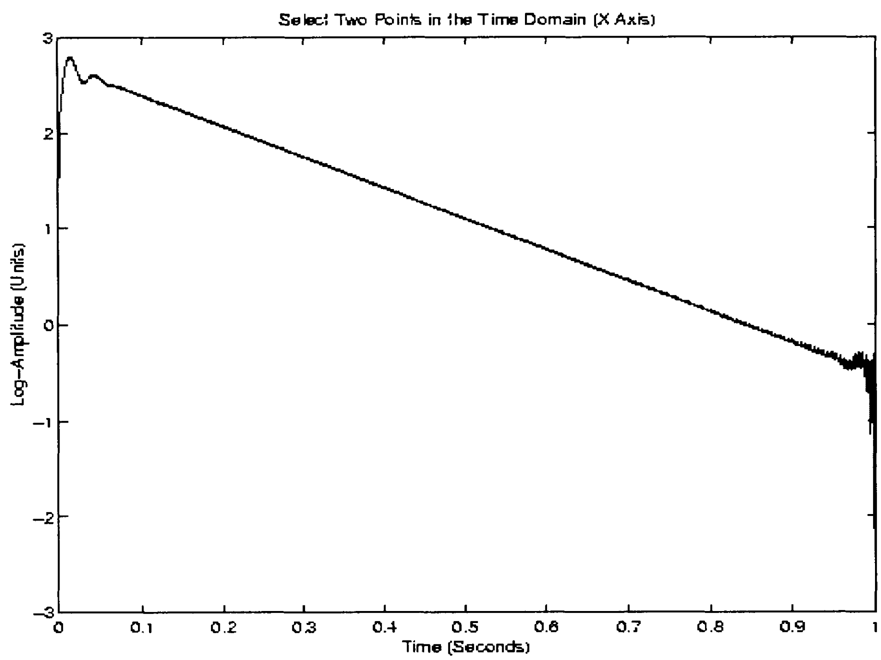


(b) The natural logarithm of the envelope plot

**Figure 4.6** (a) The envelope plot of IRF and (b) the natural logarithm of the envelope plot for the second mode (256 Hz) with lower damping ratios and no noise (SNR = $\infty$ dB)

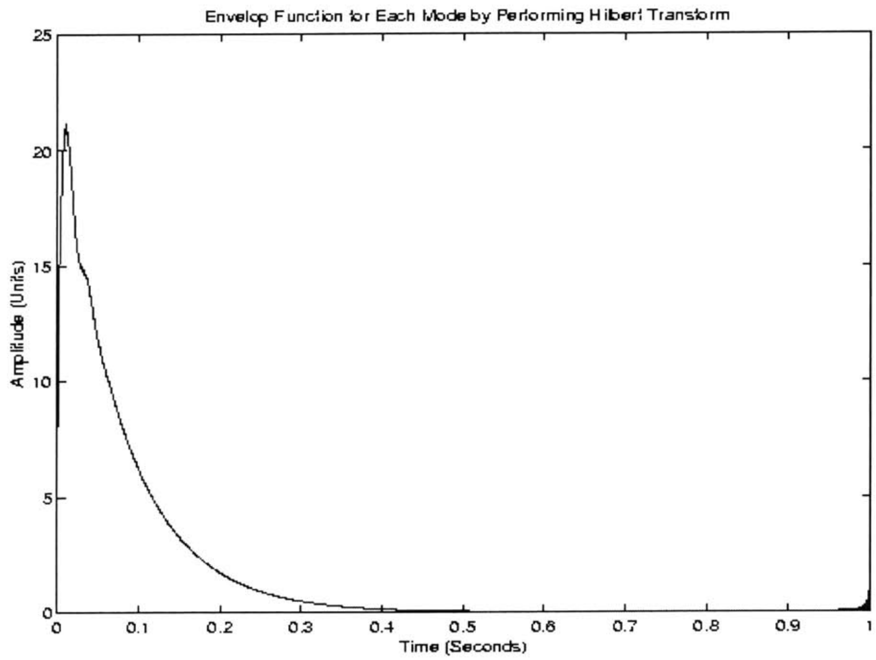


(a) The envelope plot of the recovered IRF

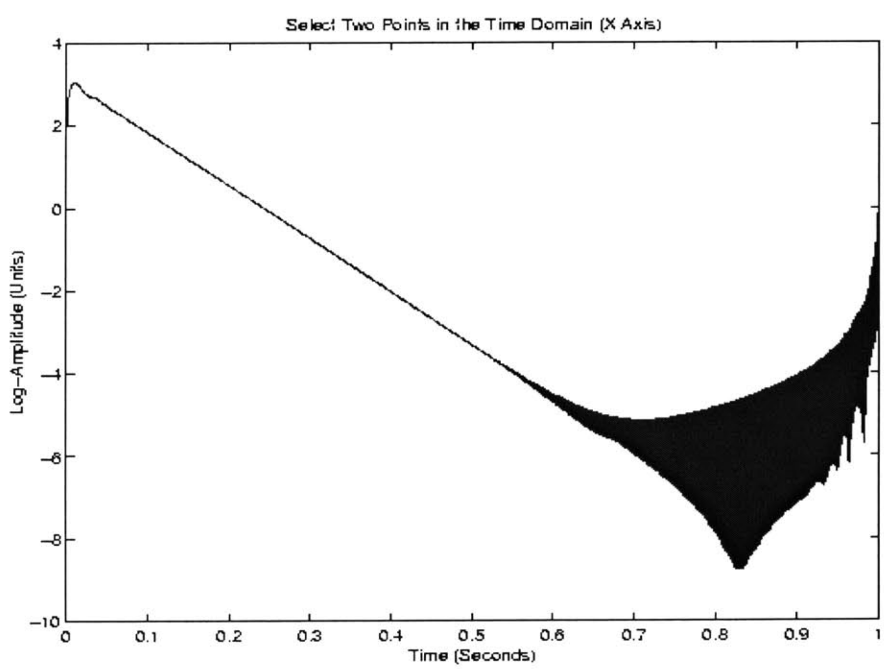


(b) The natural logarithm of the envelope plot

**Figure 4.7** (a) The envelope plot of IRF and (b) the natural logarithm of the envelope plot for the third mode (512 Hz) with lower damping ratios and no noise (SNR = $\infty$ dB)

**Table 4.5** Estimation results based on the WPM with lower damping ratios for separated modes

| Frequency (Hz) | Theoretical Value ($\zeta_t$) | SNR (dB) | Estimated Value ($\zeta_e$) | Error (%) |
|---|---|---|---|---|
| 128 | 0.0010000000 | ∞ | 0.0010002010 | 0.0 |
| | | 20 | 0.0010062009 | 0.6 |
| | | 10 | 0.0011231249 | 12.3 |
| 256 | 0.0020000000 | ∞ | 0.0020001153 | 0.0 |
| | | 20 | 0.0019535783 | -2.3 |
| | | 10 | 0.0020962840 | 4.8 |
| 512 | 0.0040000000 | ∞ | 0.0040009695 | 0.0 |
| | | 20 | 0.0039105249 | -2.2 |
| | | 10 | 0.0038905812 | -2.7 |

**Table 4.6** Estimation results based on the WPM with higher damping ratios for separated modes

| Frequency (Hz) | Theoretical Value ($\zeta_t$) | SNR (dB) | Estimated Value ($\zeta_e$) | Error (%) |
|---|---|---|---|---|
| 128 | 0.0200000000 | ∞ | 0.0199940737 | 0.0 |
| | | 20 | 0.0205325482 | 2.7 |
| | | 10 | 0.0210118603 | 5.1 |
| 256 | 0.0400000000 | ∞ | 0.0407593580 | 1.9 |
| | | 20 | 0.0460069535 | 15.0 |
| | | 10 | 0.0487173964 | 21.8 |
| 512 | 0.0800000000 | ∞ | 0.0194593050 | -75.7 |
| | | 20 | 0.0199934186 | -75.0 |
| | | 10 | 0.0738355996 | -7.7 |

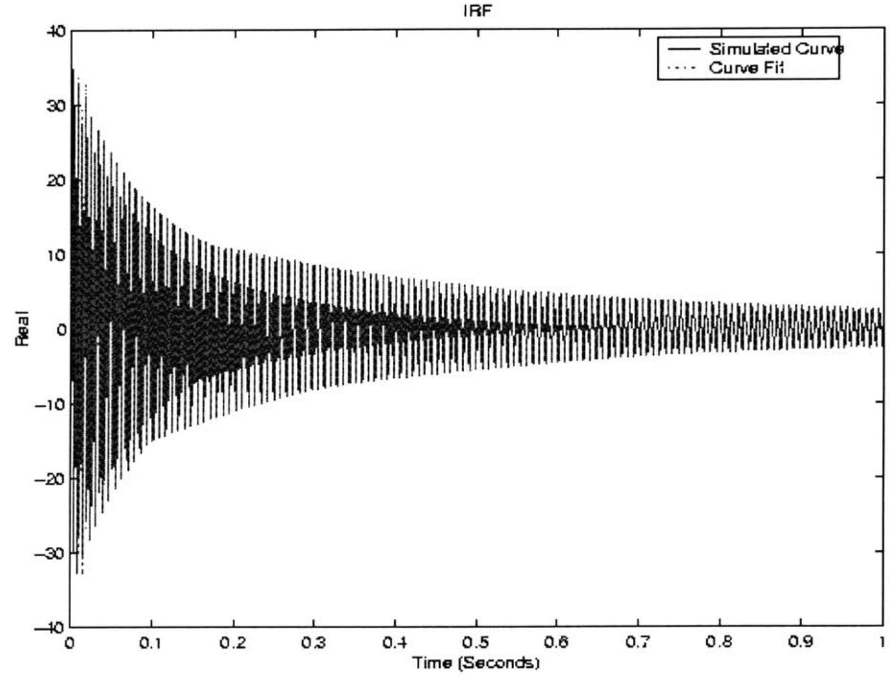


(a) IRF plot of the simulated and fitted curve

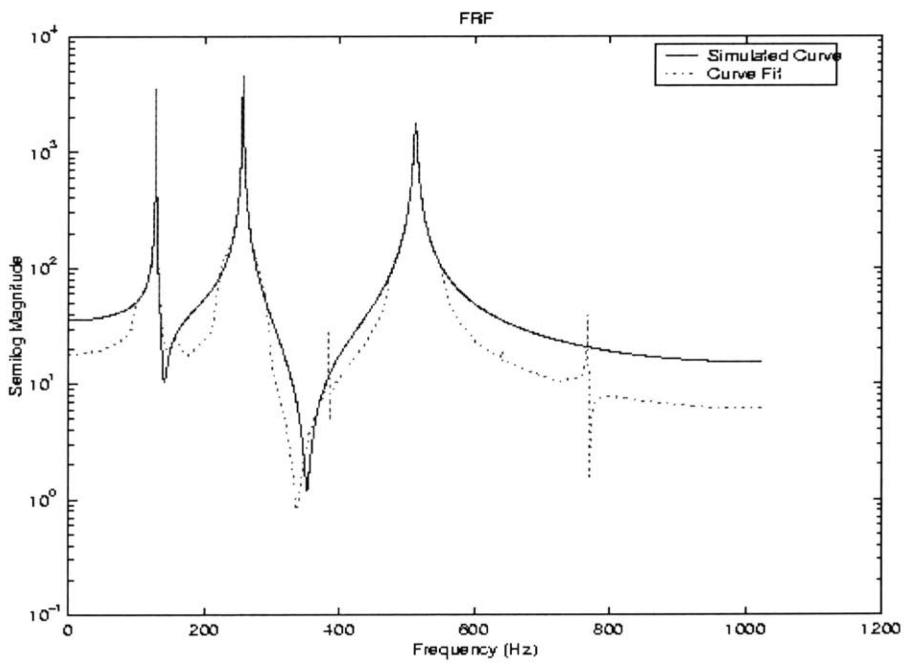


(b) FRF plot of the simulated and fitted curve

**Figure 4.8** (a) IRF and (b) FRF plot of the simulated and fitted curve with separated modes, lower damping ratios and no noise (SNR = $\infty$ dB)

### 4.1.3 CWT Results

This method first computes the pseudo-frequencies corresponding to the scales given from 0 to 60 and the wavelet function, cmor. Therefore the scales to the nearest integer 16, 8 and 4 are assigned to represent each mode because they characterize the nearest modal frequencies. Table 4.7 summarizes the corresponding scales and pseudo-frequencies of each mode. The above results can also be achieved by analyzing the plot of the continuous wavelet transform coefficients. In this thesis, the wavelet function cmor is complex and the continuous wavelet transform coefficients are complex as well. In Figure 4.9, observe that there are three brighter peaks around scale 4, 8 and 16, just like our previous computation. For each assigned scale, the magnitude of the continuous wavelet coefficients is calculated. By taking the natural logarithm of the magnitude of coefficients, a linear plot is obtained. The results are shown in Figure 4.10, 4.11 and 4.12. The Least Square Method is then applied to find the regression line. The damping ratio can be calculated from the slope of the regression line. Table 4.8 and 4.9 summarize the estimation results with lower damping ratios and higher damping ratios respectively.

**Table 4.7** Summary of corresponding scales and pseudo-frequencies for separated modes

| Frequency (Hz) | Corresponding Scale (To Nearest Integer) | Pseudo-Frequency (Hz) |
|---|---|---|
| 128 | 16 | 127.938 |
| 256 | 8 | 255.875 |
| 512 | 4 | 511.750 |

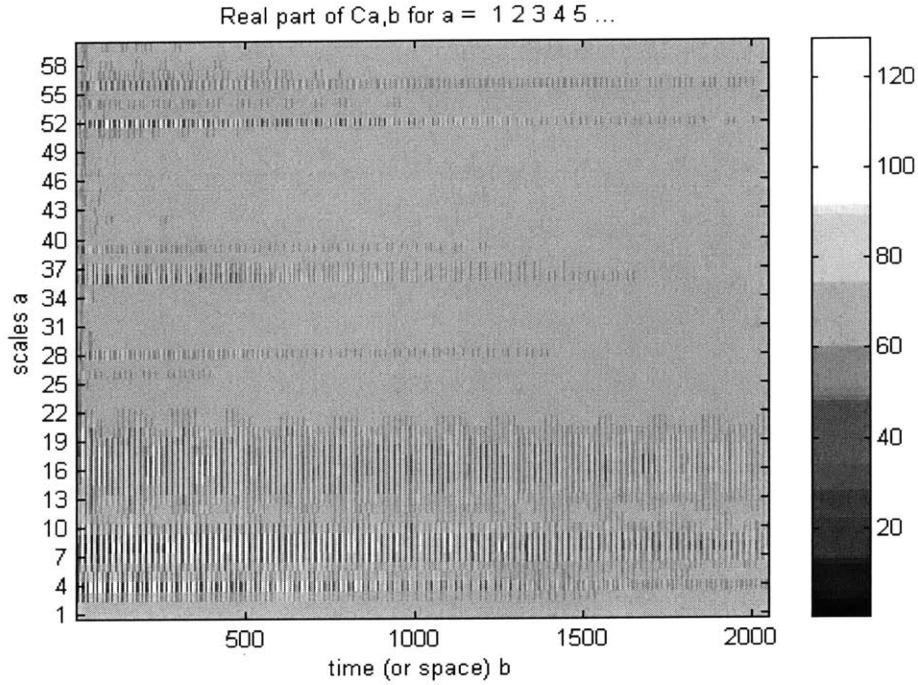


(a) Real part of continuous wavelet coefficients

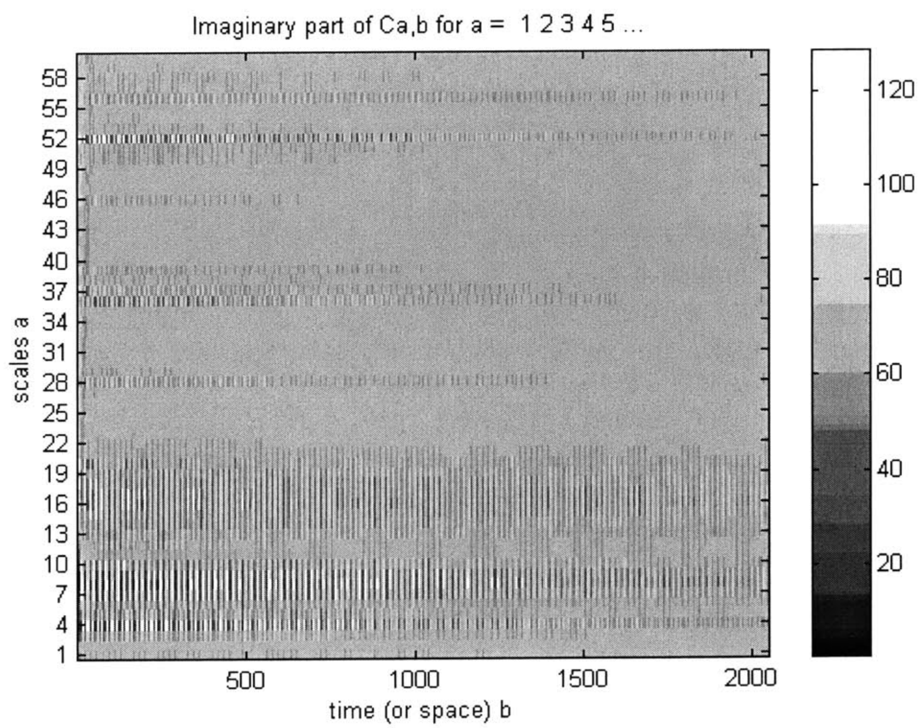


(b) Imaginary part of continuous wavelet coefficients

**Figure 4.9** (a) Real and (b) imaginary part of continuous wavelet coefficients for separated modes with lower damping ratios and no noise (SNR = $\infty$ dB)

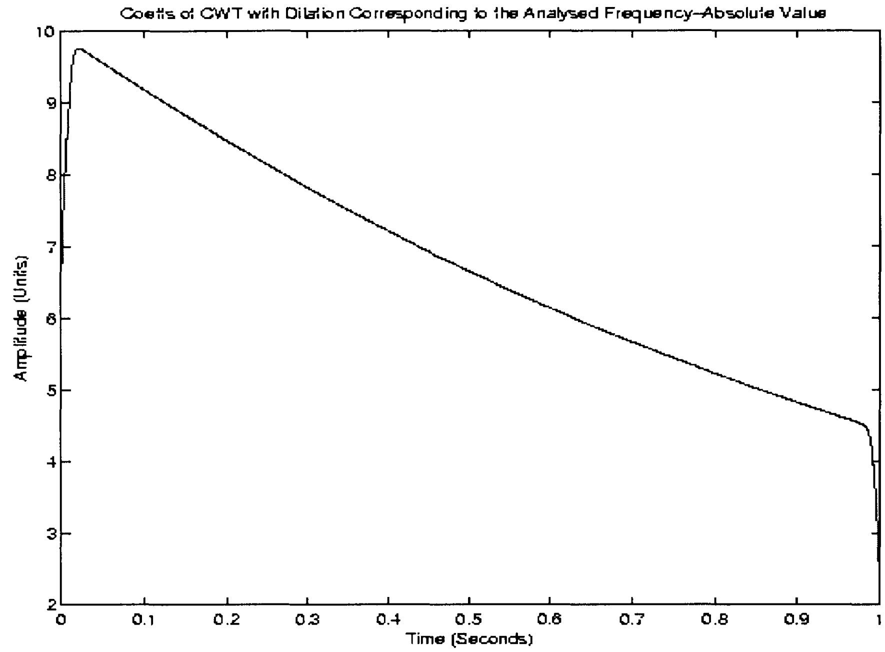


(a) The modulus plot of continuous wavelet coefficients

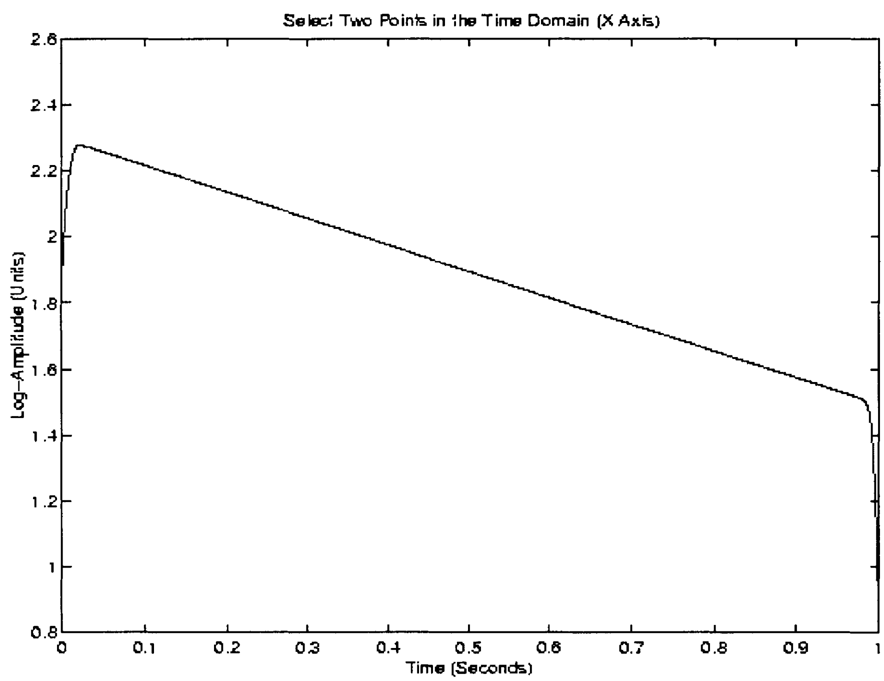


(b) The natural logarithm of the modulus of continuous wavelet coefficients

**Figure 4.10** (a) The modulus plot of continuous wavelet coefficients and (b) the natural logarithm of the modulus for the first mode (128 Hz) with lower damping ratios and no noise (SNR = $\infty$ dB)

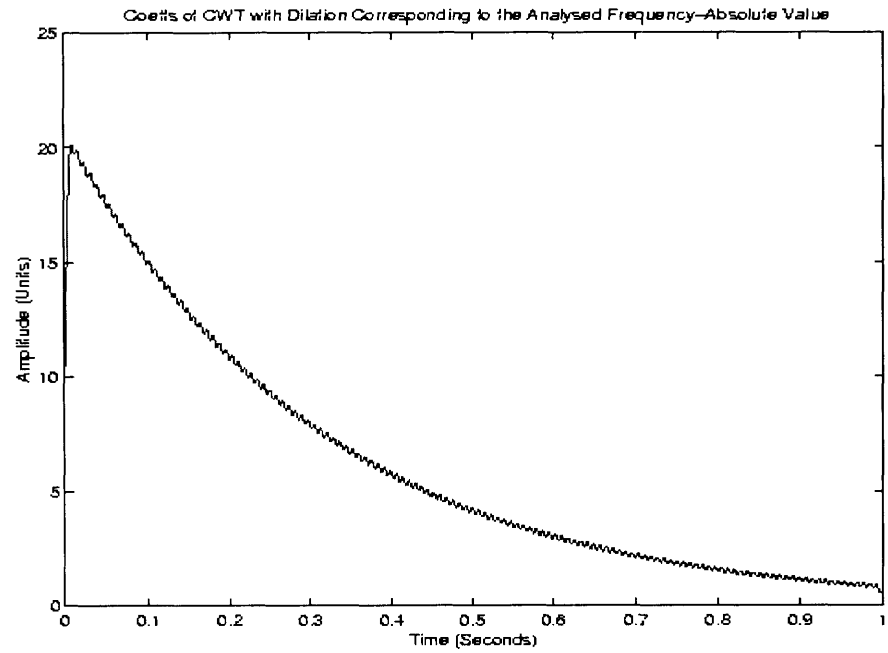


(a) The modulus plot of continuous wavelet coefficients

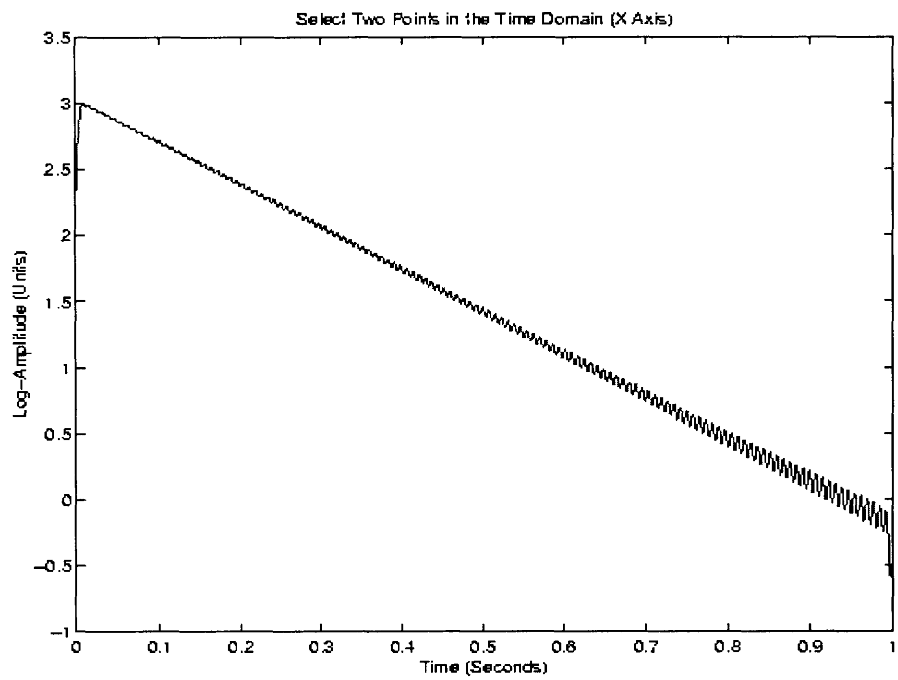


(b) The natural logarithm of the modulus of continuous wavelet coefficients

**Figure 4.11** (a) The modulus plot of continuous wavelet coefficients and (b) the natural logarithm of the modulus for the second mode (256 Hz) with lower damping ratios and no noise (SNR = $\infty$ dB)

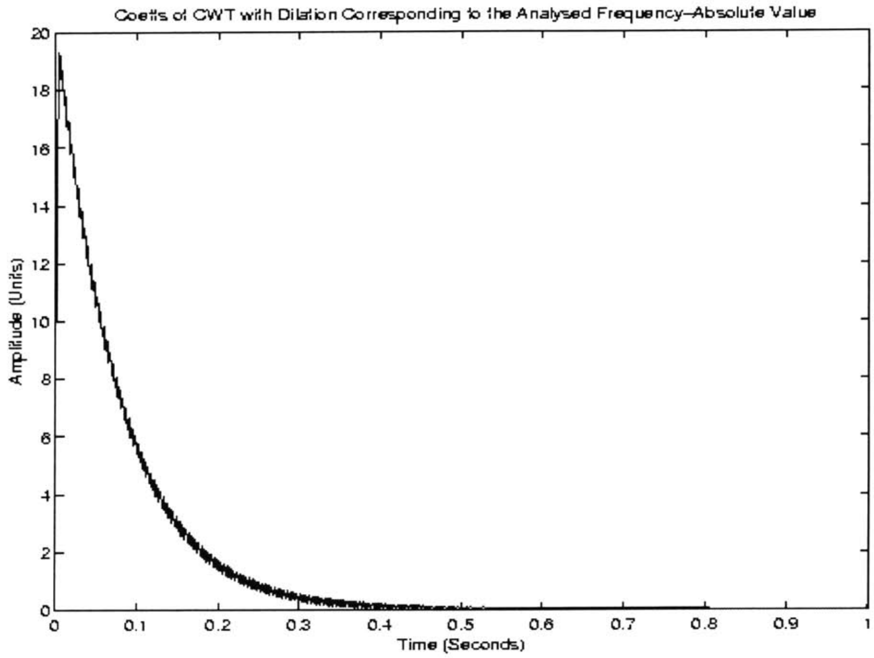


(a) The modulus plot of continuous wavelet coefficients

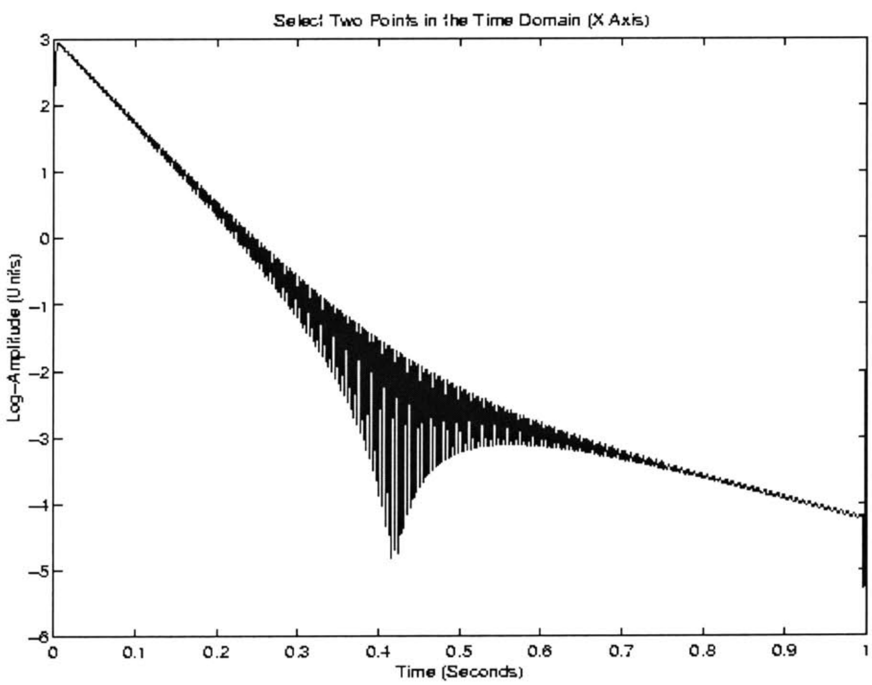


(b) The natural logarithm of the modulus of continuous wavelet coefficients

**Figure 4.12** (a) The modulus plot of continuous wavelet coefficients and (b) the natural logarithm of the modulus for the third mode (512 Hz) with lower damping ratios and no noise (SNR = $\infty$ dB)

**Table 4.8** Estimation results based on the CWT with lower damping ratios for separated modes

| Frequency (Hz) | Theoretical Value ($\zeta_t$) | SNR (dB) | Estimated Frequency (Hz) | Estimated Value ($\zeta_e$) | Error (%) |
|---|---|---|---|---|---|
| 128 | 0.0010000000 | ∞ | 127.9375 | 0.0009999992 | 0.0 |
| | | 20 | 127.9375 | 0.0010153860 | 1.5 |
| | | 10 | 127.9375 | 0.0011174334 | 11.7 |
| 256 | 0.0020000000 | ∞ | 255.8750 | 0.0020001986 | 0.0 |
| | | 20 | 255.8750 | 0.0019999981 | 0.0 |
| | | 10 | 255.8750 | 0.0019112178 | -4.4 |
| 512 | 0.0040000000 | ∞ | 511.7500 | 0.0039971511 | 0.0 |
| | | 20 | 511.7500 | 0.0040033523 | 0.1 |
| | | 10 | 511.7500 | 0.0040296956 | 0.7 |

**Table 4.9** Estimation results based on the CWT with higher damping ratios for separated modes

| Frequency (Hz) | Theoretical Value ($\zeta_t$) | SNR (dB) | Estimated Frequency (Hz) | Estimated Value ($\zeta_e$) | Error (%) |
|---|---|---|---|---|---|
| 128 | 0.0200000000 | ∞ | 127.9375 | 0.0199999989 | 0.0 |
| | | 20 | 127.9375 | 0.0210598981 | 5.3 |
| | | 10 | 127.9375 | 0.0150054876 | -25.0 |
| 256 | 0.0400000000 | ∞ | 255.8750 | 0.0403160007 | 0.8 |
| | | 20 | 255.8750 | 0.0412185046 | 3.0 |
| | | 10 | 255.8750 | 0.0383236299 | -4.2 |
| 512 | 0.0800000000 | ∞ | 511.7500 | 0.0831832863 | 3.9 |
| | | 20 | 511.7500 | 0.0849756493 | 6.2 |
| | | 10 | 511.7500 | 0.0767286681 | -4.1 |

### 4.1.4 Discussion

CEM: The results demonstrate that the accuracy of estimation is adversely affected when the FRF is truncated. For example in the case of the third mode without noisy data (SNR=$\infty$dB) for lower damping ratios, the percentage error surges from 0% to −17.6% (Table 4.1). For the cases without truncation, the results are only good (0%) when there is no noisy data and are affected significantly by adding the noisy data in the signal. The percentage error is usually too high to be accepted in the cases with noisy data. We can also observe that the method gives better estimations for higher modes and cases with higher damping ratios (Table 4.2 and 4.3).

WPM: The results show good accuracy of estimation even for the data corrupted by the noise. It fails only in the cases of the third mode for higher damping ratios (Table 4.6). By decreasing the SNR from $\infty$dB to 10dB in the case of the second mode for lower damping ratios, the percentage error slightly deviates from 0% to 4.8% (Table 4.5). There are two factors influencing the accuracy of estimations: the selected nodes and the time ranges for the Least Square Method. Because of disturbances at the beginning and end of the plot of natural logarithm, choosing suitable time ranges gives a better regression line. Other observations are that the method performs better for lower damping ratios (Table 4.5 and 4.6) and the fitted curve in Figure 4.8 is not a perfect reconstruction because only the effects of the selected nodes are considered.

CWT: The results show better accuracy of estimation even for the data corrupted by the noise. By decreasing the SNR from $\infty$dB to 10dB in the case of the second mode for lower damping ratios, the percentage error slightly deviates from 0% to –4.4% (Table 4.8). Other observations are that choosing time ranges for the

Least Square Method affects the accuracy of estimation as well and the method performs better for lower damping ratios (Table 4.8 and 4.9).

## 4.2 Simulated Analytical Signal With Close Modes

This part summarizes the results of the three methods by analyzing the signal with close modes. The frequencies corresponding to the close modes are 256, 307.2, 399.36 (Hz). Other parameters in the signal are defined in Chapter 3.

### 4.2.1 CEM Results

Table 4.10 summarizes the results without truncation. Figure 4.13 shows the IRF, FRF and phase angle plot of the simulated and fitted curves with lower damping ratios and noisy data (SNR = 20 dB).

**Table 4.10** Estimation results based on the CEM for close modes

| Frequency (Hz) | Theoretical Value ($\zeta_t$) | SNR (dB) | Estimated Value ($\zeta_e$) | Error (%) |
|---|---|---|---|---|
| 256 | 0.0010000000 | ∞ | 0.0009999997 | 0.0 |
| | | 20 | 0.1395905363 | 13859.1 |
| | | 10 | 0.1031841278 | 10218.4 |
| 307.2 | 0.0012000000 | ∞ | 0.0012000006 | 0.0 |
| | | 20 | 0.0214321119 | 1686.0 |
| | | 10 | 0.1076112707 | 8867.6 |
| 399.36 | 0.0015600000 | ∞ | 0.0015599998 | 0.0 |
| | | 20 | 0.0109457636 | 601.7 |
| | | 10 | 0.0519293293 | 3228.8 |

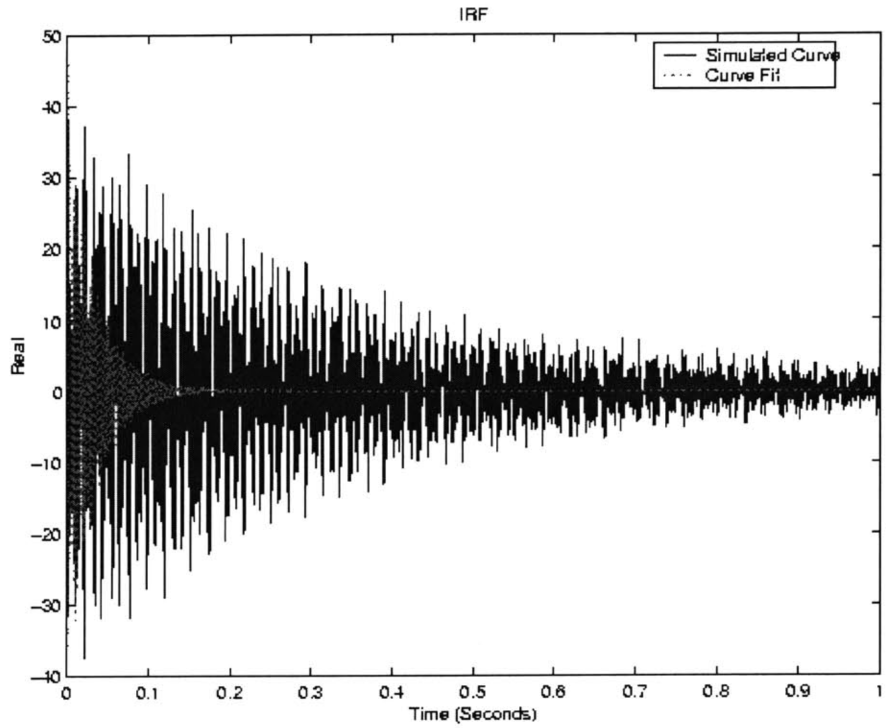


(a) IRF plot of the simulated and fitted curve

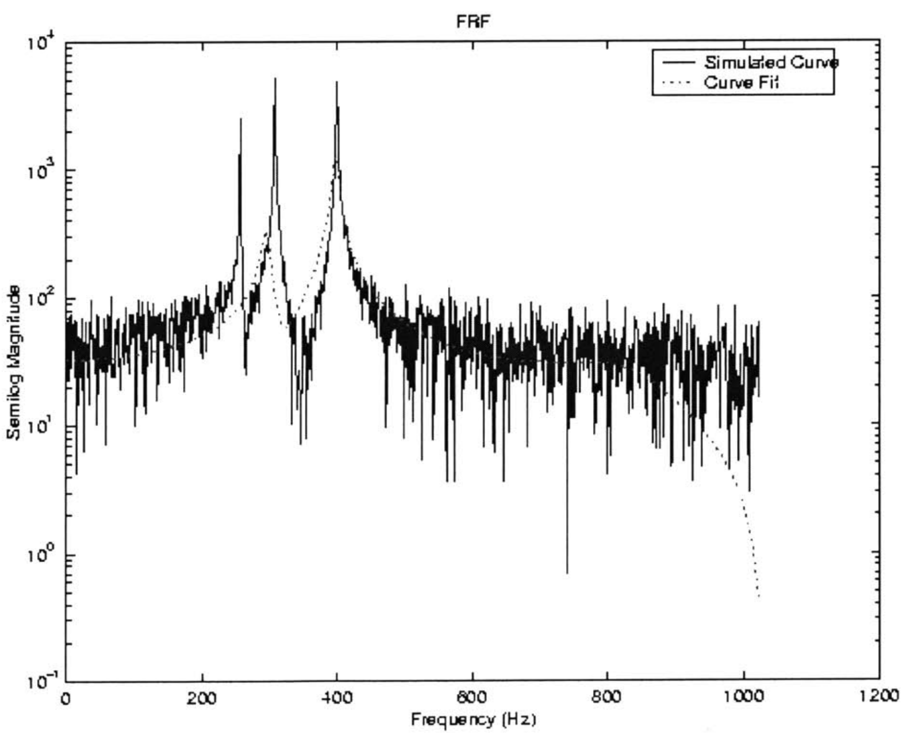

(b) FRF plot of the simulated and fitted curve

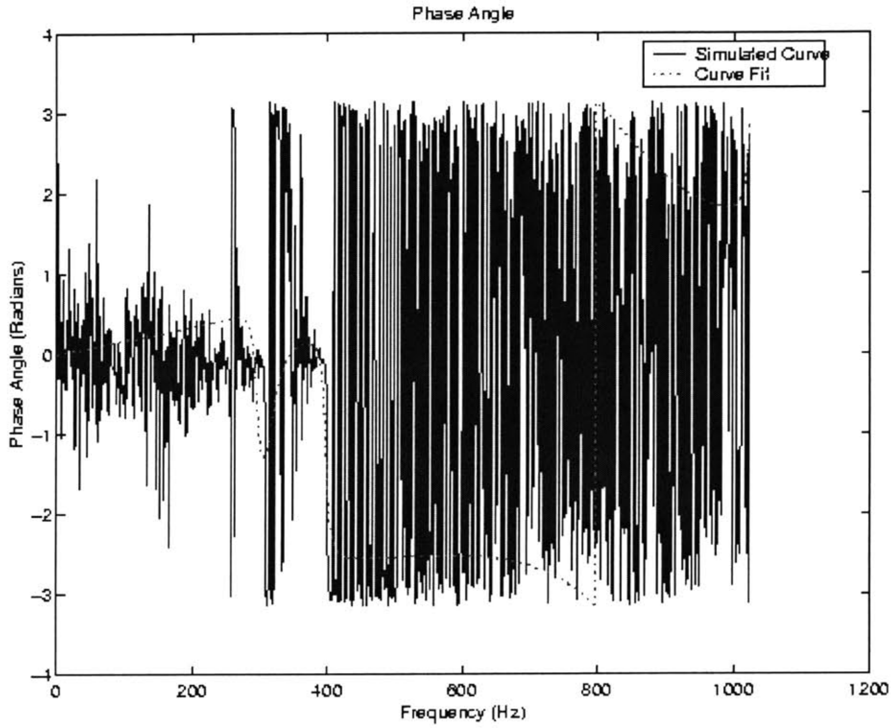


(c) Phase angle plot of the simulated and fitted curve

**Figure 4.13** (a) IRF, (b) FRF and (c) phase angle plot of the simulated and fitted curve with close modes and noisy data (SNR = 20 dB)

## 4.2.2 WPM Results

The same procedure as in section 4.1.2 can be followed to extract damping ratios. The FRF of selected nodes are shown in Figure 4.14, 4.15 and 4.16. Table 4.11 summarizes the selected nodes corresponding to the three modes. Figure 4.17, 4.18 and 4.19 show the results of mode response after taking the Hilbert transform and natural logarithm. Figure 4.20 shows the IRF and FRF of the simulated and fitted curve with lower damping ratios and no noise added. Table 4.12 summarizes the estimation results.

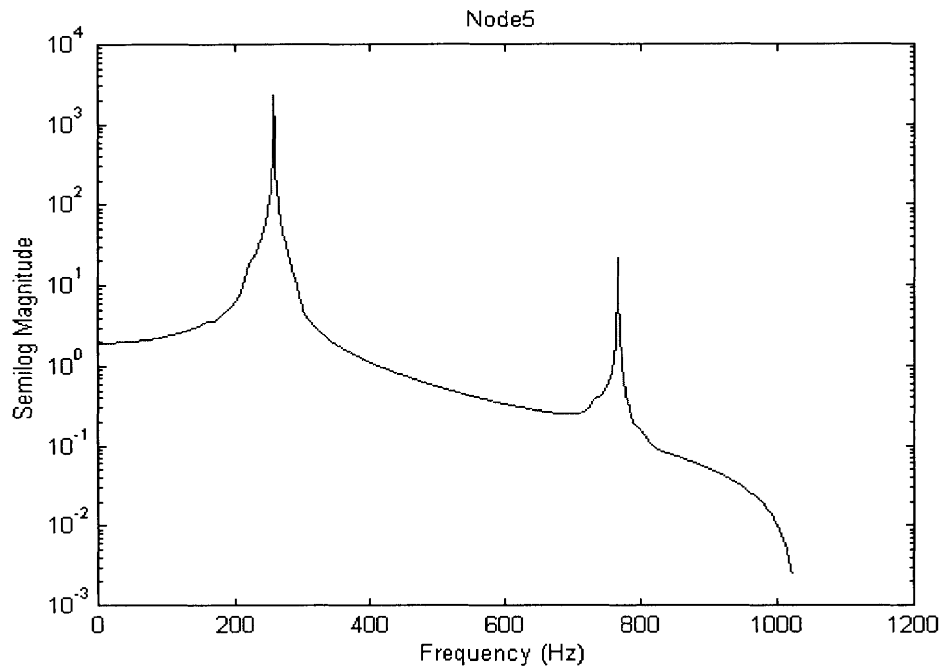


(a) FRF plot of wavelet packet node 5

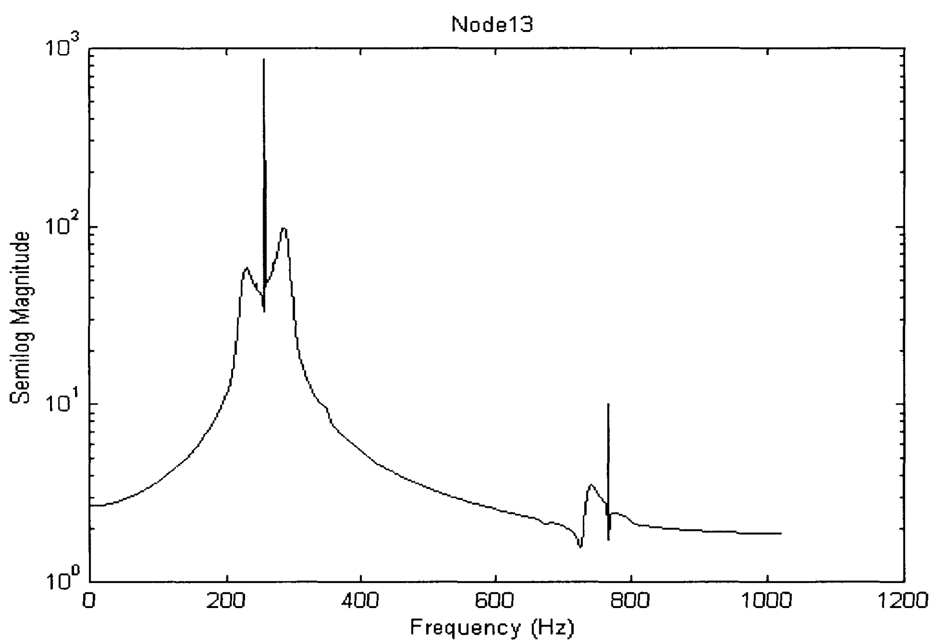


(b) FRF plot of wavelet packet node 13

**Figure 4.14** (a) FRF plot of wavelet packet node 5 and (b) node 13 representing the first mode (256 Hz) without noisy data (SNR = $\infty$ dB)

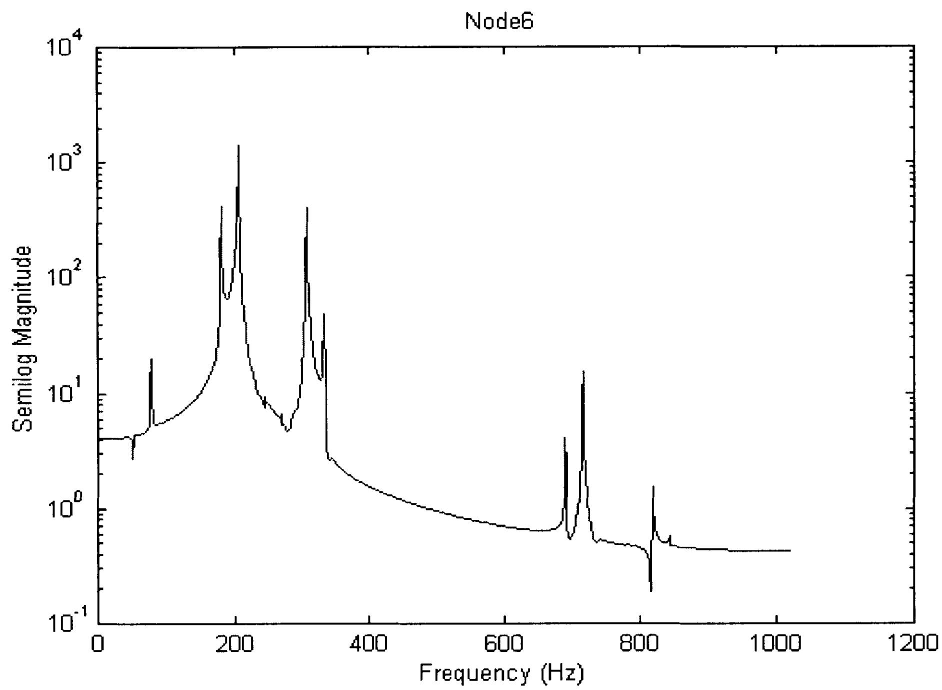


(a) FRF plot of wavelet packet node 6

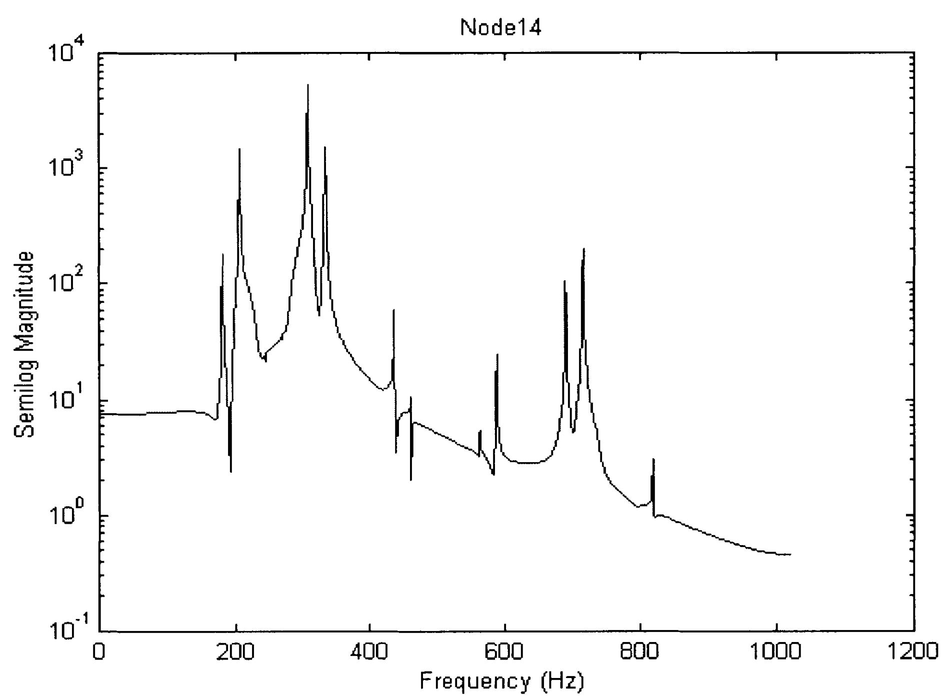


(b) FRF plot of wavelet packet node 14

**Figure 4.15** (a) FRF plot of wavelet packet node 6 and (b) node 14 representing the second mode (307.2 Hz) without noisy data (SNR = $\infty$ dB)

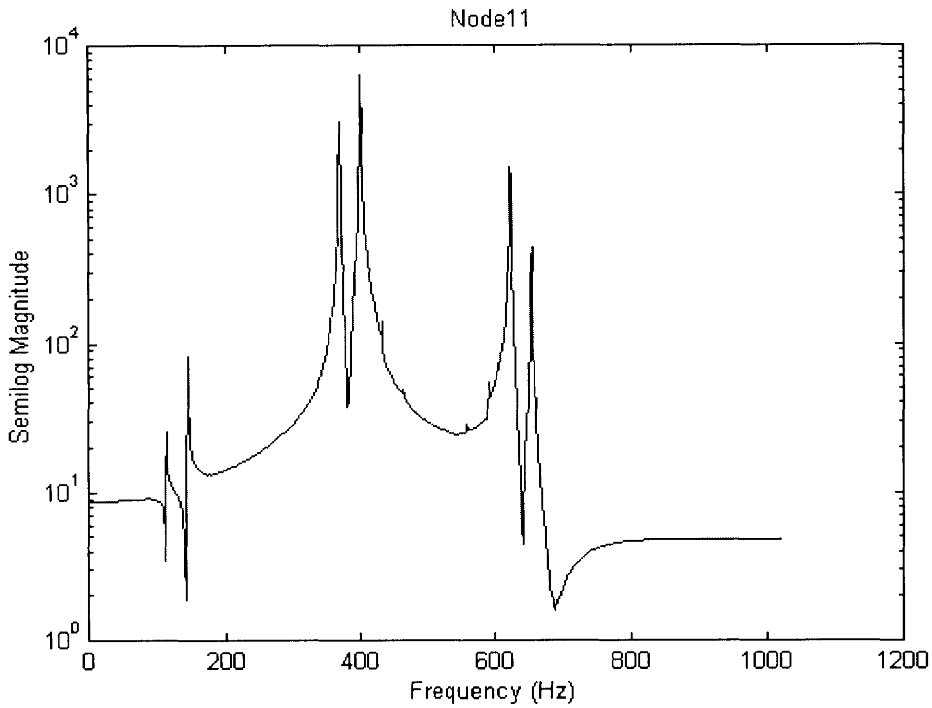


(a) FRF plot of wavelet packet node 11

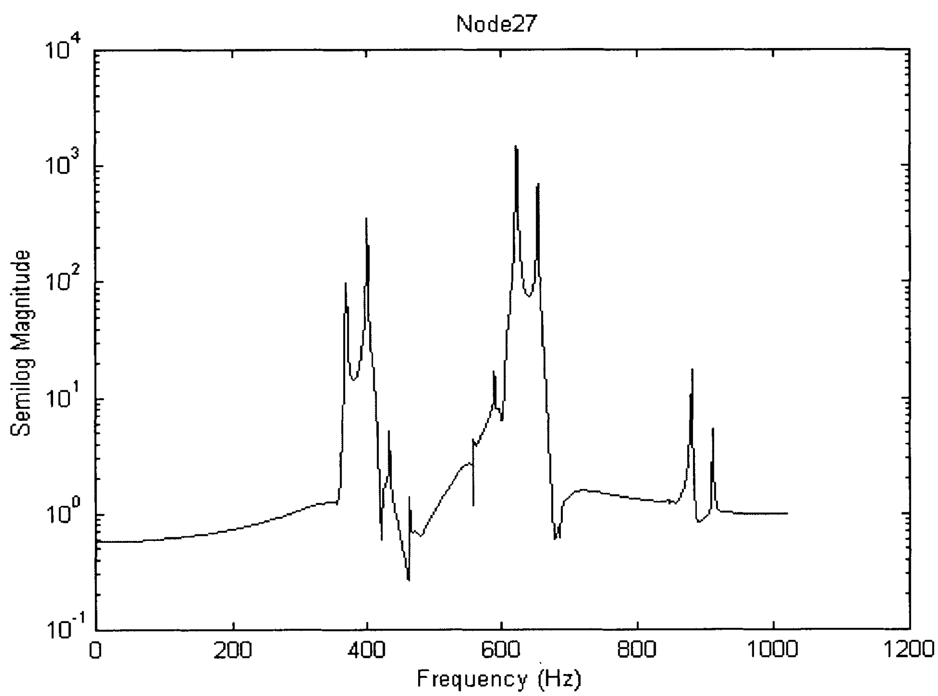


(b) FRF plot of wavelet packet node 27

**Figure 4.16** (a) FRF plot of wavelet packet node 11 and (b) node 27 representing the third mode (399.36 Hz) without noisy data (SNR = $\infty$ dB)

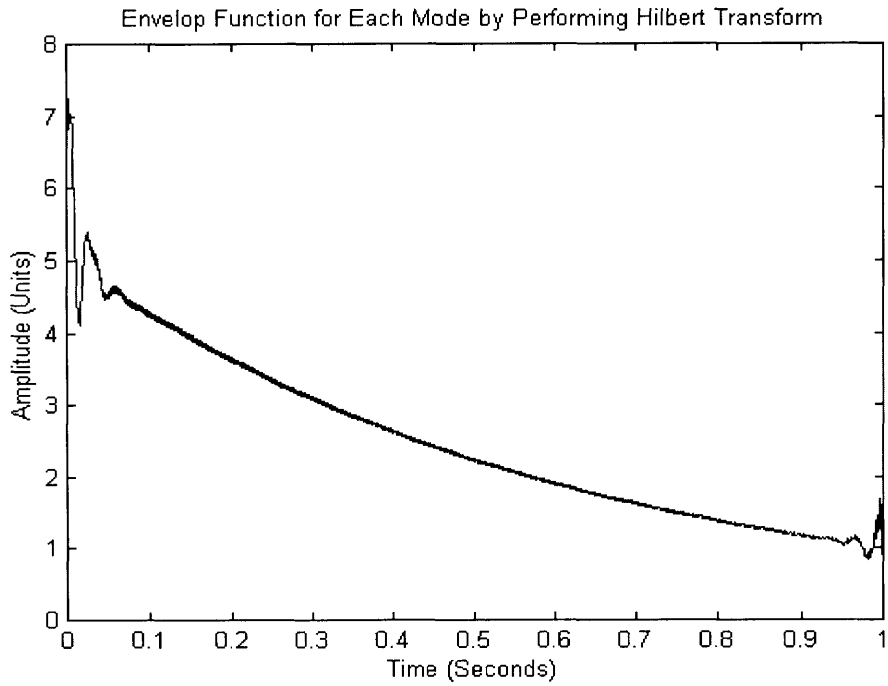


(a) The envelope plot of the recovered IRF

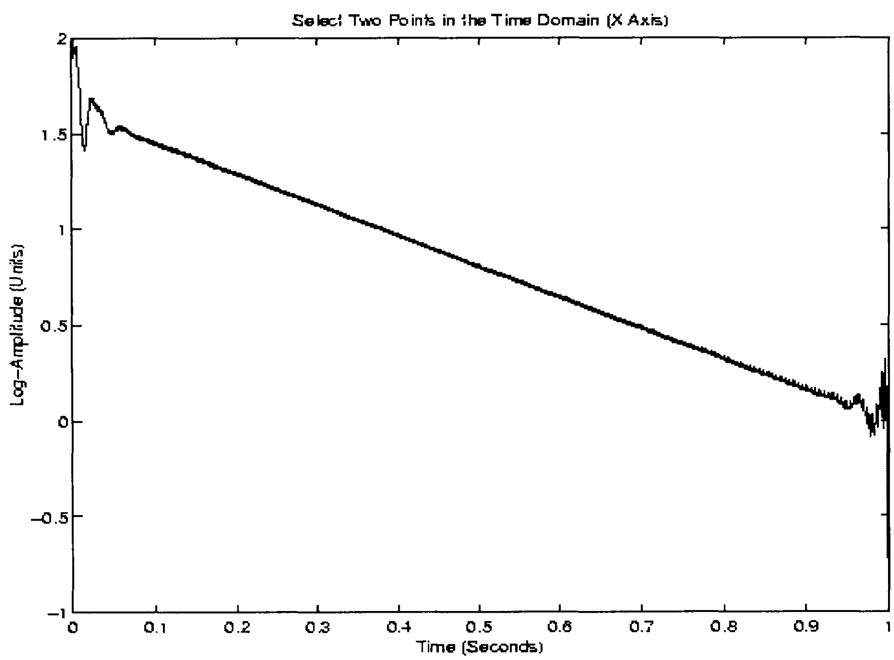


(b) The Natural logarithm of the envelope plot

**Figure 4.17** (a) The envelope plot of IRF and (b) the natural logarithm of the envelope plot for the first mode (256 Hz) without noisy data (SNR = $\infty$ dB)

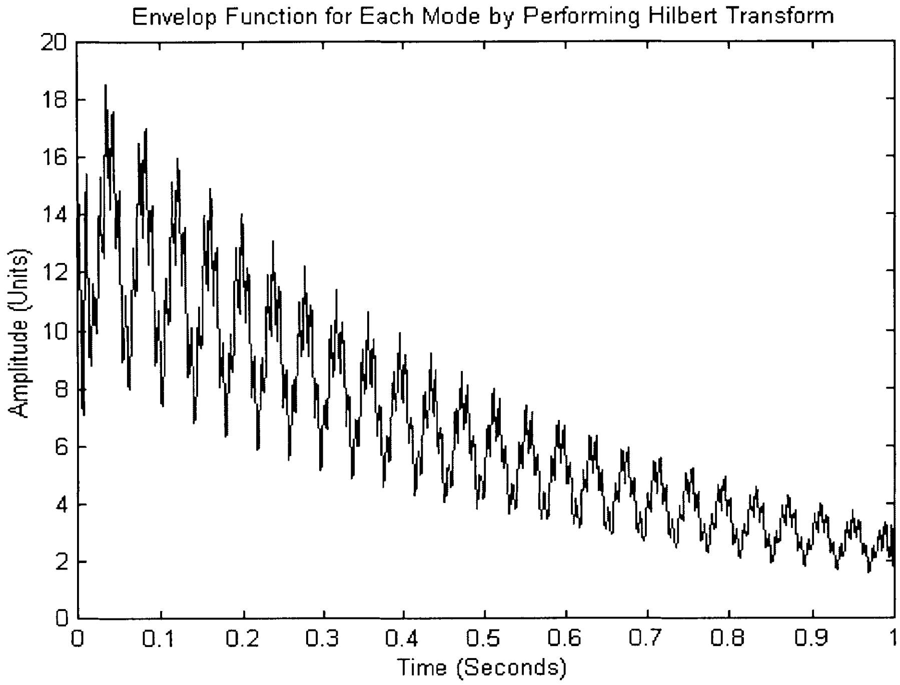


(a) The envelope plot of the recovered IRF

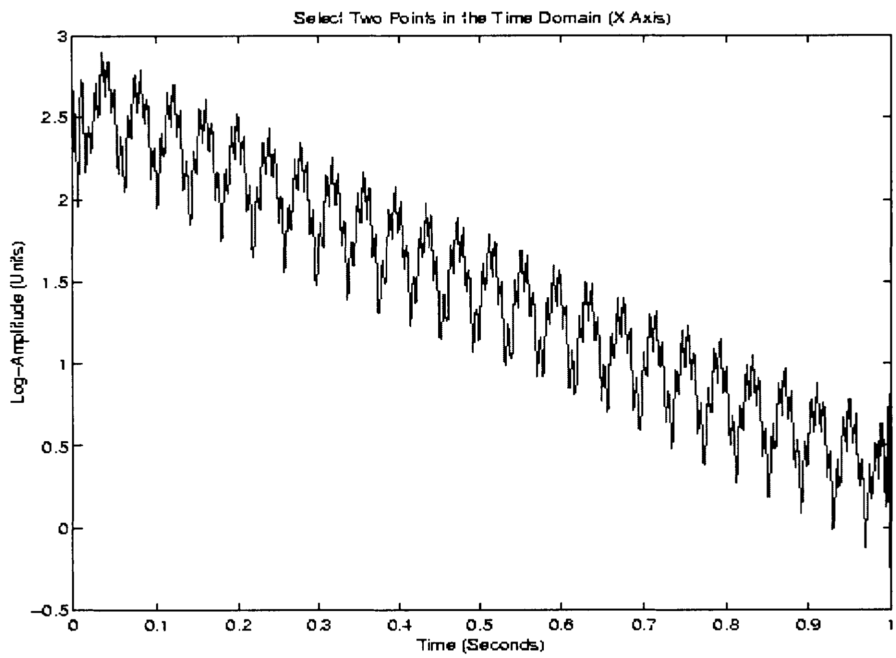


(b) The Natural logarithm of the envelope plot

**Figure 4.18** (a) The envelope plot of IRF and (b) the natural logarithm of the envelope plot for the second mode (307.2 Hz) without noisy data (SNR = $\infty$ dB)

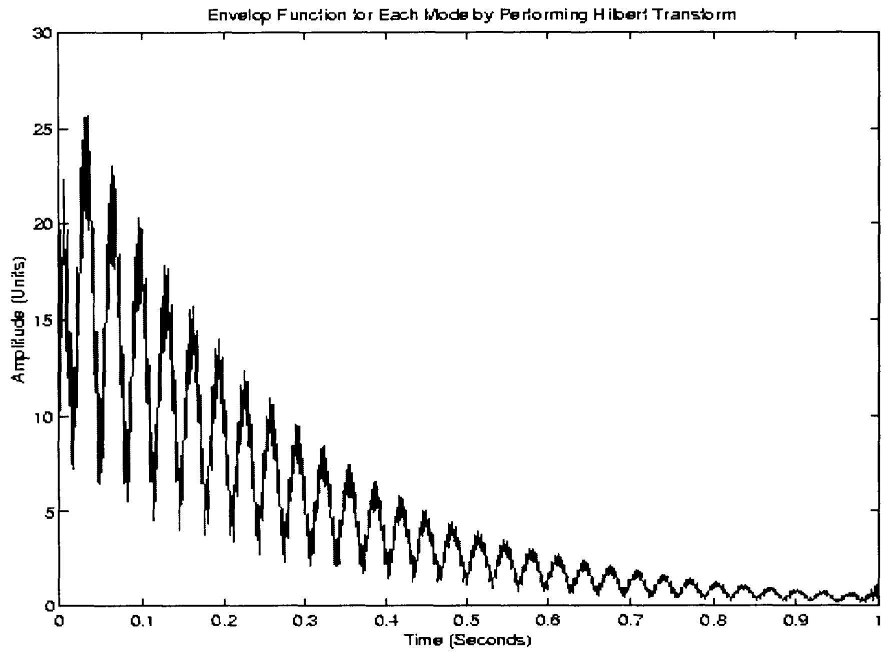


(a) The envelope plot of the recovered IRF

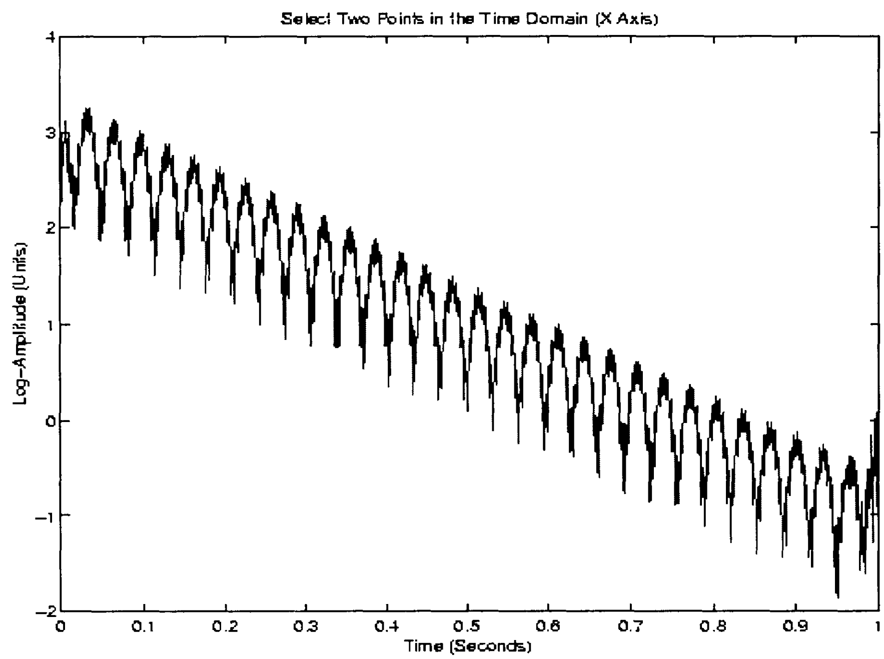


(b) The Natural logarithm of the envelope plot

**Figure 4.19** (a) The envelope plot of IRF and (b) the natural logarithm of the envelope plot for the third mode (399.36 Hz) without noisy data (SNR = $\infty$ dB)

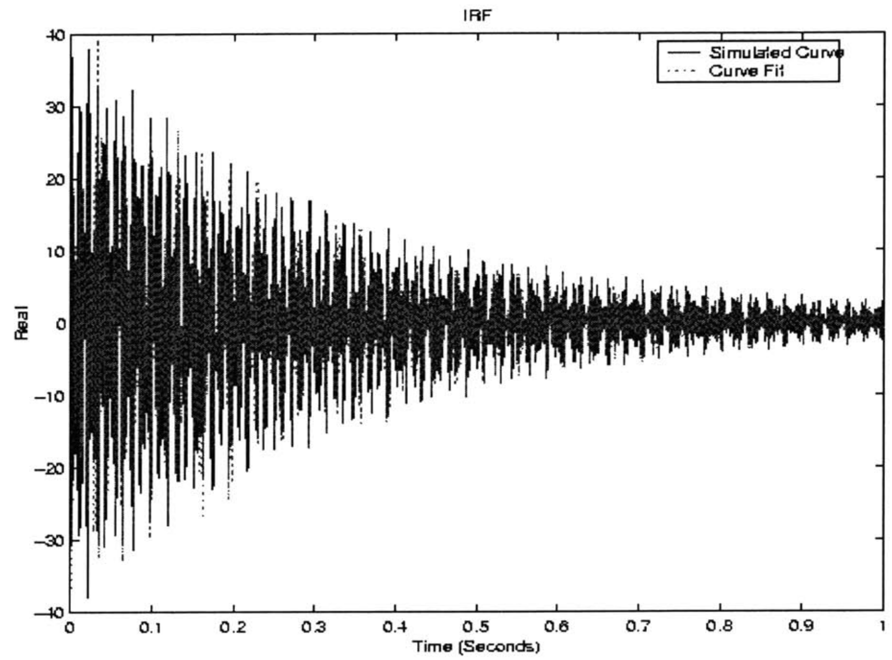


(a) IRF plot of the simulated and fitted curve

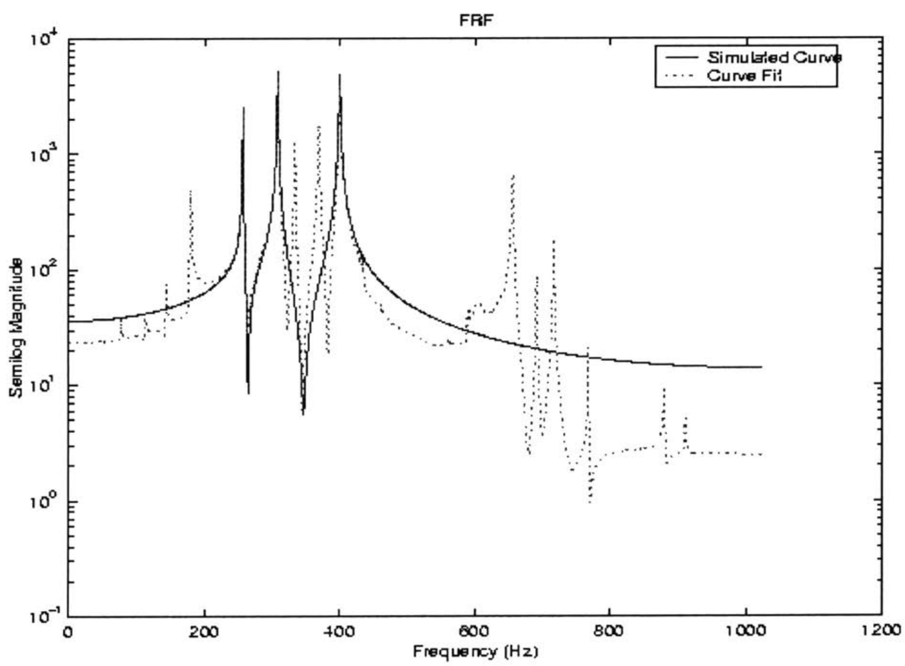


(b) FRF plot of the simulated and fitted curve

**Figure 4.20** (a) IRF and (b) FRF plot of the simulated and fitted curve with close modes and no noise (SNR = $\infty$ dB)

**Table 4.11** Summary of selected nodes corresponding to three close modes

| Frequency (Hz) | Relative Nodes |
|---|---|
| 256 | Node(5), Node(13) |
| 307.2 | Node(6), Node(14) |
| 399.36 | Node(11), Node(27) |

**Table 4.12** Estimation results based on the WPM for close modes

| Frequency (Hz) | Theoretical Value ($\zeta_t$) | SNR (dB) | Estimated Value ($\zeta_e$) | Error (%) |
|---|---|---|---|---|
| 256 | 0.0010000000 | $\infty$ | 0.0009999698 | 0.0 |
| | | 20 | 0.0010103531 | 1.0 |
| | | 10 | 0.0008083364 | -19.2 |
| 307.2 | 0.0012000000 | $\infty$ | 0.0012056756 | 0.5 |
| | | 20 | 0.0012120838 | 1.0 |
| | | 10 | 0.0010319571 | -14.0 |
| 399.36 | 0.0015600000 | $\infty$ | 0.0015610941 | 0.1 |
| | | 20 | 0.0015280909 | -2.0 |
| | | 10 | 0.0015548646 | -0.3 |

### 4.2.3 CWT Results

The same procedure as in section 4.1.3 can be followed to extract damping ratios. Table 4.13 summarizes the corresponding scales and pseudo-frequencies of each mode. Figure 4.21 shows the continuous wavelet coefficients. Figure 4.22, 4.23 and 4.24 show the modulus plot of continuous wavelet coefficients and the natural logarithm of the modulus. Table 4.14 summarizes the estimation results with lower damping ratios.

**Table 4.13** Summary of corresponding scales and pseudo-frequencies for close modes

| Frequency (Hz) | Corresponding Scale (To Nearest Integer) | Pseudo-Frequency (Hz) |
|---|---|---|
| 256 | 8 | 255.8750 |
| 307.2 | 7 | 292.4285 |
| 399.36 | 5 | 409.4000 |

**Table 4.14** Estimation results based on the CWT for close modes

| Frequency (Hz) | Theoretical Value ($\zeta_t$) | SNR (dB) | Estimated Frequency (Hz) | Estimated Value ($\zeta_e$) | Error (%) |
|---|---|---|---|---|---|
| 256 | 0.0010000000 | ∞ | 255.8750 | 0.0014256900 | 42.6 |
| | | 20 | 255.8750 | 0.0013769379 | 37.7 |
| | | 10 | 255.8750 | 0.0012866067 | 28.7 |
| 307.2 | 0.0012000000 | ∞ | 292.4285 | 0.0011897881 | -0.9 |
| | | 20 | 292.4285 | 0.0011776139 | -1.9 |
| | | 10 | 292.4285 | 0.0011617518 | -3.2 |
| 399.36 | 0.0015600000 | ∞ | 409.4000 | 0.0015658358 | 0.4 |
| | | 20 | 409.4000 | 0.0015502614 | -0.6 |
| | | 10 | 409.4000 | 0.0015241656 | -2.3 |

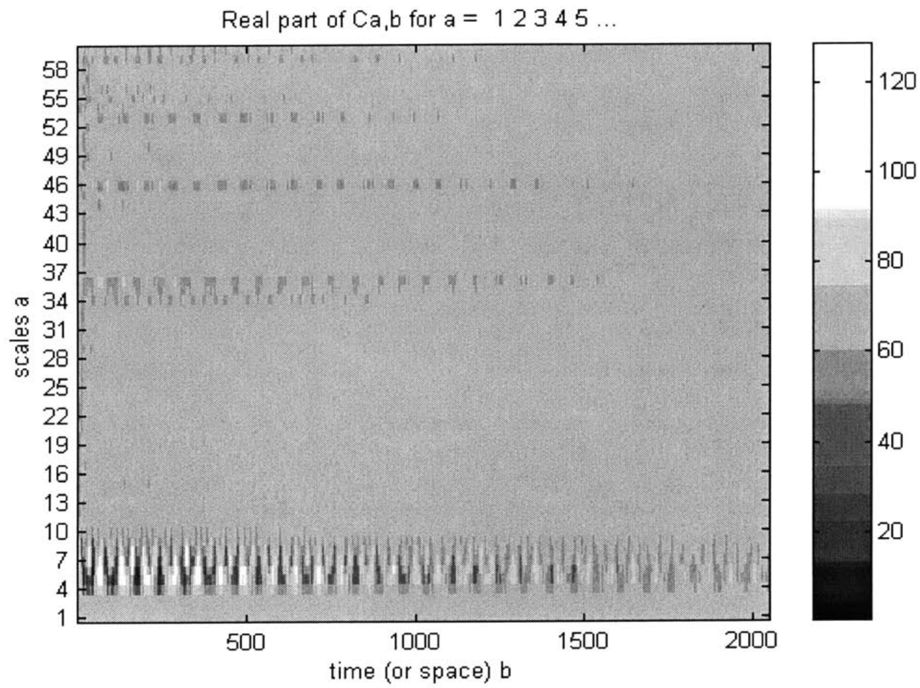


(a) Real part of continuous wavelet coefficients

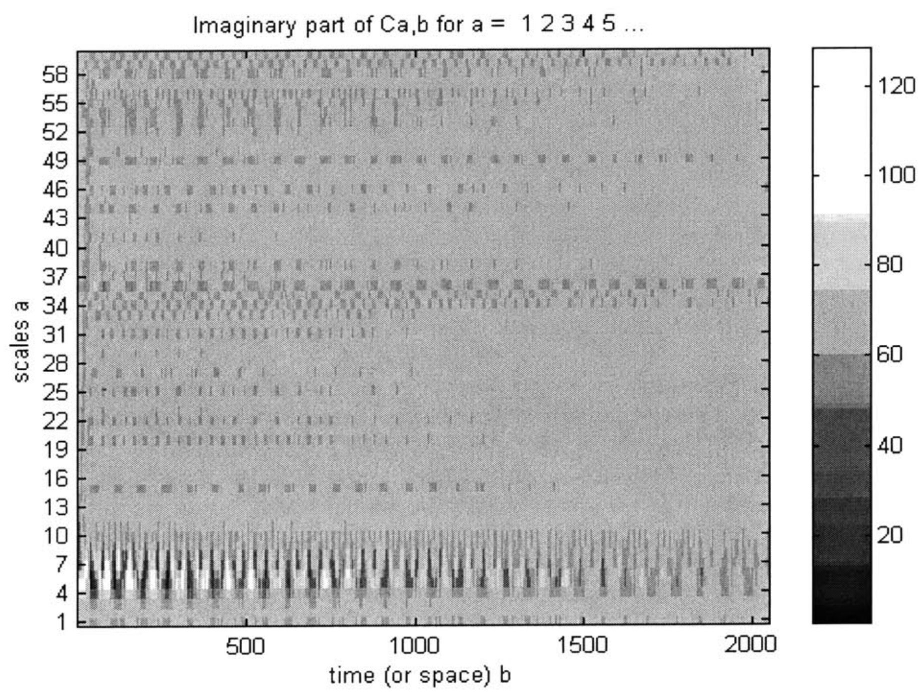


(b) Imaginary part of continuous wavelet coefficients

**Figure 4.21** (a) Real and (b) imaginary part of continuous wavelet coefficients for close modes without noisy data (SNR = $\infty$ dB)

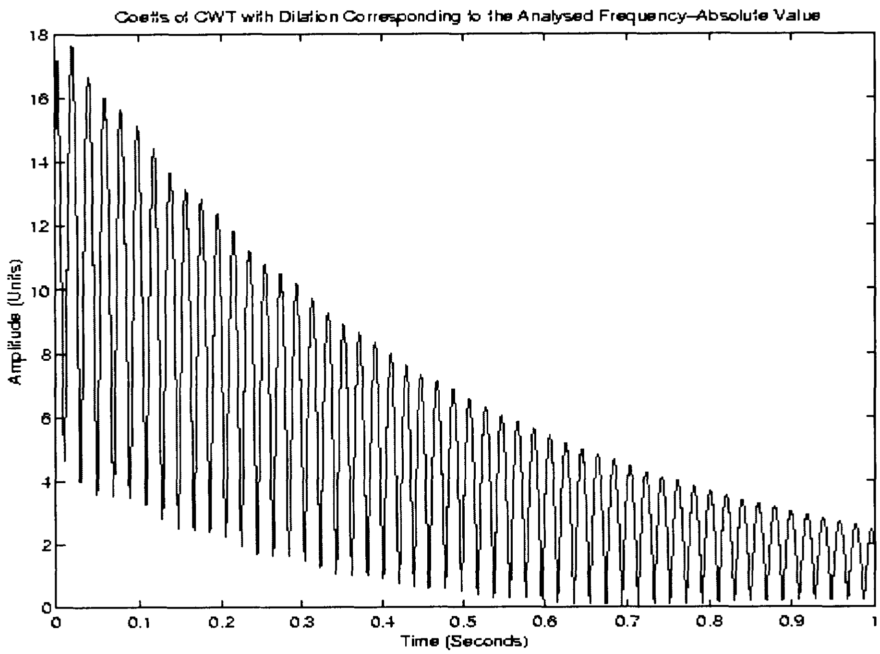


(a) The modulus plot of continuous wavelet coefficients

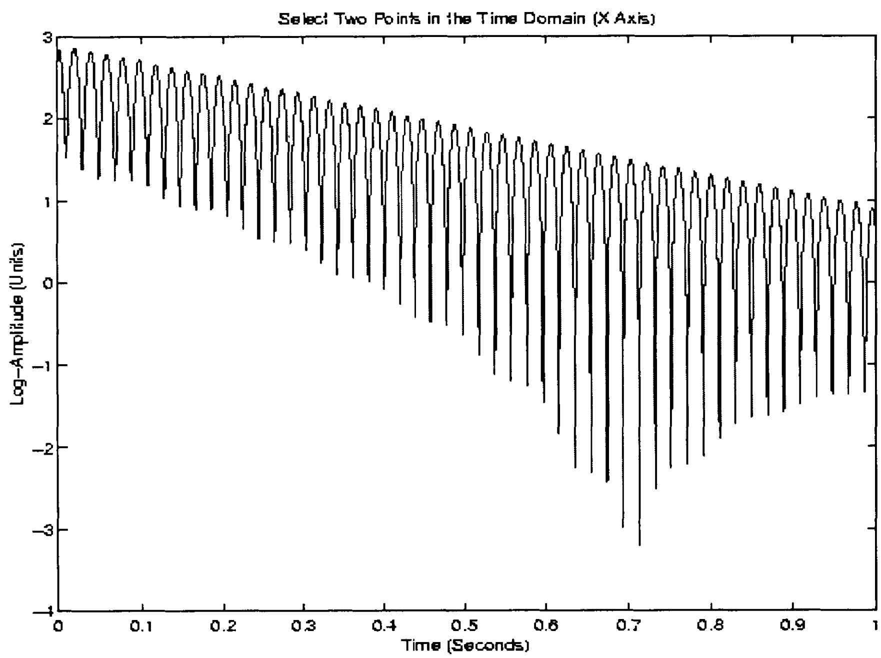


(b) The natural logarithm of the modulus of continuous wavelet coefficients

**Figure 4.22** (a) The modulus plot of continuous wavelet coefficients and (b) the natural logarithm of the modulus for the first mode (256 Hz) without noisy data (SNR = $\infty$ dB)

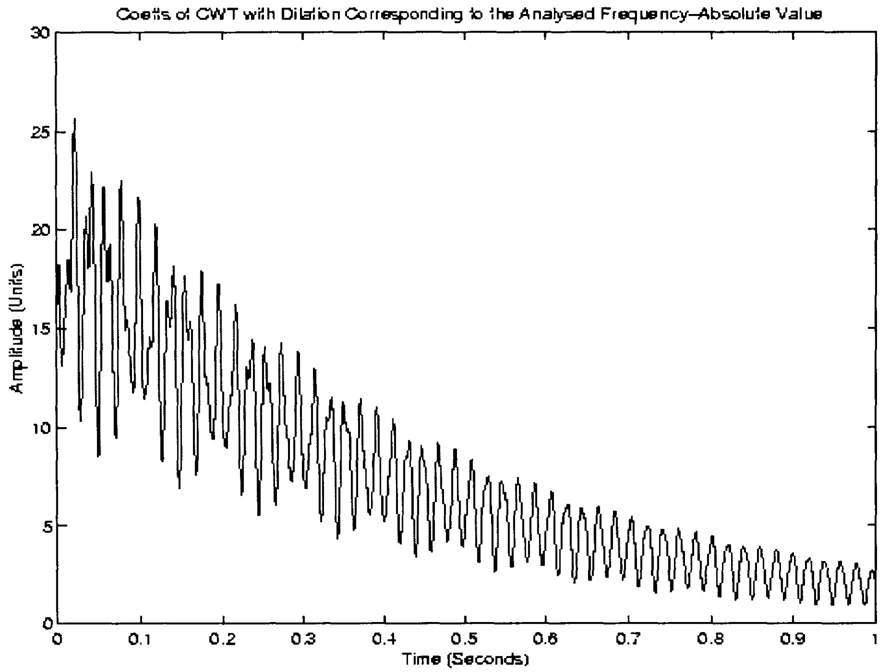


(a) The modulus plot of continuous wavelet coefficients

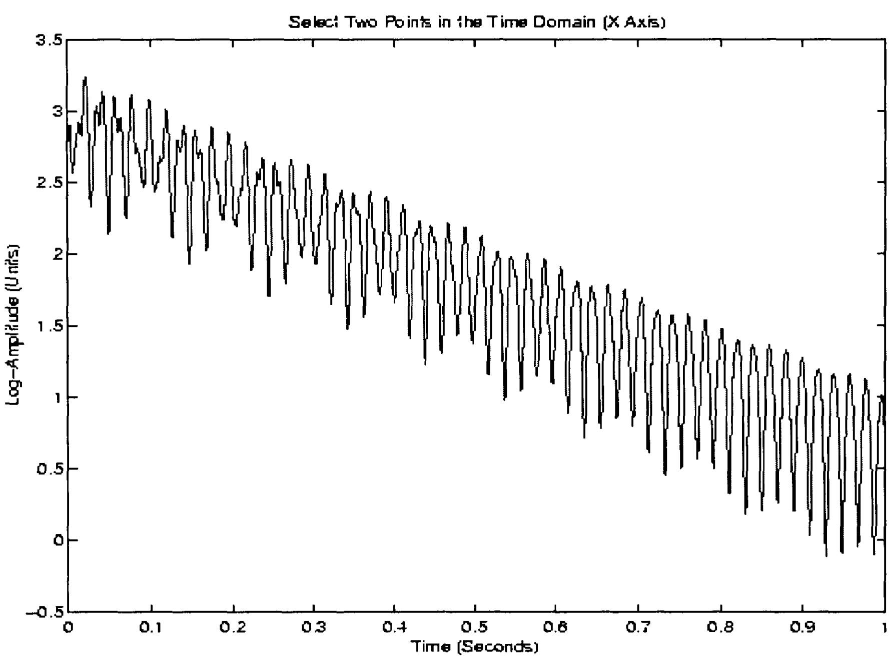


(b) The natural logarithm of the modulus of continuous wavelet coefficients

**Figure 4.23** (a) The modulus plot of continuous wavelet coefficients and (b) the natural logarithm of the modulus for the second mode (307.2 Hz) without noisy data (SNR = $\infty$ dB)

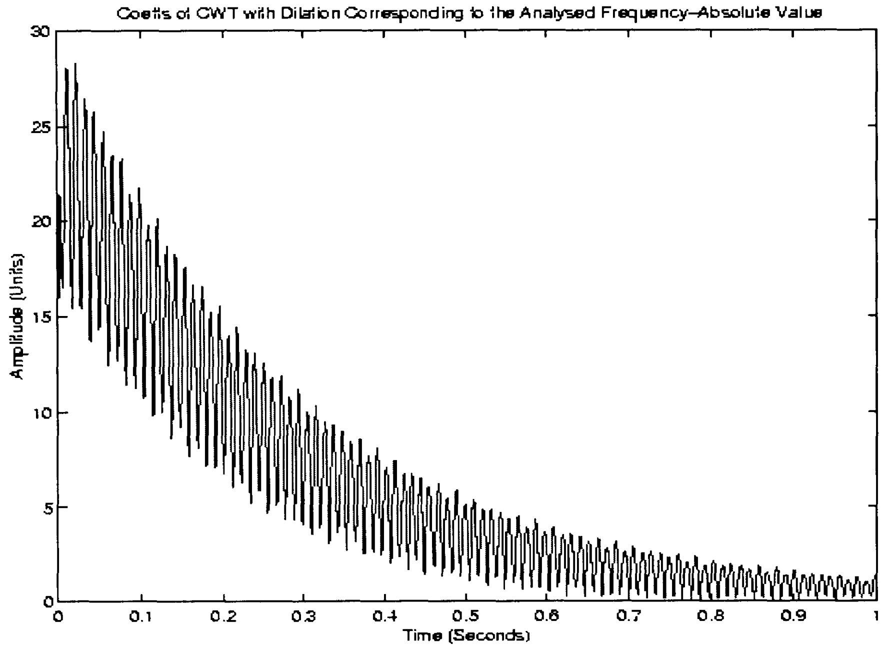


(a) The modulus plot of continuous wavelet coefficients

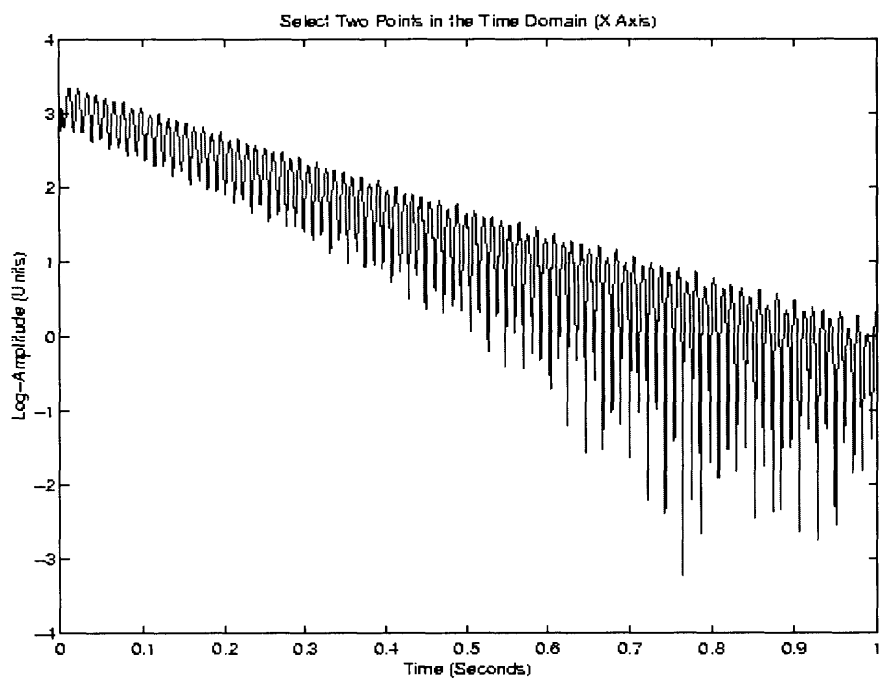


(b) The natural logarithm of the modulus of continuous wavelet coefficients

**Figure 4.24** (a) The modulus plot of continuous wavelet coefficients and (b) the natural logarithm of the modulus for the third mode (399.36 Hz) without noisy data (SNR = $\infty$ dB)

### 4.2.4 Discussion

CEM: The results demonstrate good accuracy of estimation without noisy data. In the presence of noisy data, it affects the results significantly. We can also observe that the method gives better estimations for higher modes (Table 4.10).

WPM: The results show less accuracy of estimation compared to the cases based on WPM with separated modes but the error remains less than 10% except for the case with noisy data (SNR=10 dB) (Table 4.12). There exist more oscillations in the envelope plot of the recovered IRF as shown in Figure 4.18 and 4.19. The problem could be the overlap of the close modal frequencies within the bandwidth of wavelet packet bases. Therefore it becomes more crucial to choose the suitable time ranges for the Least Square Method to obtain better regression line or use a decomposition with higher than 5 levels to improve.

CWT: The results show that less accuracy of estimations of the first mode compared to the cases with separated modes but the error remains less than 5% for the other two modes (Table 4.14). The problem could be frequency selectivity of the mother wavelet is not good enough. There also exist more oscillations in the modulus plot of continuous wavelet coefficients as shown in Figure 4.22, 4.23 and 4.24. It may be improved by choosing the suitable values of the parameters, $\alpha$ and $w_0$, of the mother wavelet to give it a narrower bandwidth.

# Chapter 5
# Summary

## 5.1 Conclusion

Three methods of extracting damping ratios have been presented. Based on the results in Chapter 4, the following conclusions can be made.

1. The CWT method gives the most accurate estimations even for data corrupted by the noise. The worst is the CEM method.
2. The CEM method gives better results in the cases with higher modes and higher damping ratios. One disadvantage of this method appears to be its sensitivity to noise.
3. The WPM and CWT methods perform slightly better in the cases for extracting lower damping ratios than those for higher damping ratios, even for data corrupted by the noise.
4. The estimation results are more accurate in the cases with separated modes than those with close modes.

## 5.2 Recommendation

The recommendations to improve the frequency selectivity using the same wavelets are more levels for the WPM method and different parameters ($\alpha$, $w_0$) of the mother wavelet for the CWT method.

Future work on this topic would most certainly involve the use of other wavelets. There is a great possibility that other wavelets would lead to more accurate damping ratio measurement.

The methods also have yet to be applied to experimental data. In this thesis only simulated analytic signals with known parameters are considered.

# Appendix A

## The Complex-Exponential Method

In the frequency domain, the frequency response function (FRF) in terms of receptance $\alpha_{jk}$ (displacement at point $j$ due to a force at point $k$) for a linear, viscously damped system with N degrees of freedom (DOF) can be given by [2]

$$\alpha_{jk}(w) = \sum_{r=1}^{N}\left(\frac{{}_rA_{jk}}{w_r\zeta_r + i\left(w - w_r\sqrt{(1-\zeta_r^2)}\right)} + \frac{{}_rA_{jk}^*}{w_r\zeta_r + i\left(w + w_r\sqrt{(1-\zeta_r^2)}\right)}\right) \tag{A.1}$$

where $w_r$ is the natural frequency, $\zeta_r$ is the damping ratio, ${}_rA_{jk}$ is the residue corresponding to each mode r and * denotes complex conjugate. Another way of writing equation (A.1) is

$$\alpha_{jk}(w) = \sum_{r=1}^{2N}\frac{{}_rA_{jk}}{w_r\zeta_r + i(w - w_r^{'})} \tag{A.2}$$

where

$$w_r^{'} = w_r\sqrt{(1-\zeta_r^2)}$$

$$w_{r+N}^{'} = -w_r^{'}$$

$${}_{r+N}A_{jk} = {}_rA_{jk}^* \tag{A.3}$$

The Complex-Exponential Method (CEM) [2][3] works with the corresponding impulse response function (IRF), obtained from equation (A.2) by an inverse Fourier transform

$$h_{jk}(t) = \sum_{r=1}^{2N} {}_rA_{jk}e^{s_rt} \tag{A.4}$$

or, simply

$$h(t) = \sum_{r=1}^{2N} A_r^{'} e^{s_r t} \tag{A.5}$$

where $s_r = -w_r \zeta_r + iw_r^{'}$ and the properties in equation (A.3) hold. The time response $h(t)$ (real-valued) at a series of L equally spaced time intervals, $\Delta t$, is

$$h_0 = h(0) = \sum_{r=1}^{2N} A_r^{'}$$

$$h_1 = h(\Delta t) = \sum_{r=1}^{2N} A_r^{'} e^{s_r (\Delta t)}$$

$$\vdots$$

$$h_L = h(L.\Delta t) = \sum_{r=1}^{2N} A_r^{'} e^{s_r (L \cdot \Delta t)} \tag{A.6}$$

or, simply

$$h_0 = \sum_{r=1}^{2N} A_r^{'}$$

$$h_1 = \sum_{r=1}^{2N} A_r^{'} V_r$$

$$\vdots$$

$$h_L = \sum_{r=1}^{2N} A_r^{'} V_r^L \tag{A.7}$$

with

$$V_r = e^{s_r \Delta t} \tag{A.8}$$

The roots $s_r$ for an underdamped system always occur in complex conjugate parts, so do the modified variable $V_r$. Thus, there always exists a polynomial in $V_r$ of order $L$ with real coefficients $\beta$ (called the autoregressive coefficients) such that the following relation is verified

$$\beta_0 + \beta_1 V_r + \beta_2 V_r^2 + \cdots + \beta_L V_r^L = 0 \tag{A.9}$$

In order to calculate the coefficients $\beta_j$ to evaluate $V_r$, multiply both sides of equation (A.7) by $\beta_0$ to $\beta_L$ and sum the result. This procedure gives

$$\sum_{j=0}^{L} \beta_j h_j = \sum_{j=0}^{L} \left( \beta_j \sum_{r=1}^{2N} A_r^{'} V_r^j \right) = \sum_{r=1}^{2N} \left( A_r^{'} \sum_{j=0}^{L} \beta_j V_r^j \right) \tag{A.10}$$

The inner summation in the right side of equation (A.10) is exactly the polynomial in equation (A.9). Therefore, that summation is going to be equal to zero for each value of $V_r$, it follows that

$$\sum_{j=0}^{L} \beta_j h_j = 0 \text{, for each } V_r \tag{A.11}$$

From equation (A.11), it will be possible to calculate the coefficients $\beta_j$ ($h_j$ is measured). These coefficients are used to calculate the $V_r$, and are calculated as follows: we make $M = L/2$, and $n = 2 * DOF$. There will be n sets of data points $h_j$, each set shifted one time interval, and $\beta_L$ is assumed equal to 1. This gives

$$\begin{bmatrix} h_0 & h_1 & h_2 & \cdots & h_{n-1} \\ h_1 & h_2 & h_3 & \cdots & h_n \\ \vdots & \vdots & \vdots & \ddots & \vdots \\ h_{M-1} & h_M & h_{M+1} & \vdots & h_{n+M-2} \end{bmatrix} \begin{Bmatrix} \beta_0 \\ \beta_1 \\ \vdots \\ \beta_{n-1} \end{Bmatrix} = -\begin{Bmatrix} h_n \\ h_{n+1} \\ \vdots \\ h_{n+M-1} \end{Bmatrix} \tag{A.12}$$

or, simply

$$\underset{M\times n}{[h]}\underset{n\times 1}{\{\beta\}} = \underset{M\times 1}{\{h'\}} \tag{A.13}$$

From this equation it is possible to calculate $\{\beta\}$, as $[h]$ and $\{h'\}$ are known matrices. This can be done using pseudo-inverse technique, multiply by $[h]^T$ (transpose), and then solve for $\{\beta\}$. The result is

$$\{\beta\} = \left([h]^T [h]\right)^{-1} \left([h]^T \{h'\}\right) \tag{A.14}$$

After calculating $\{\beta\}$, it is used to calculate the $V_r$. In order to calculate the natural frequencies, and damping ratios, equation (A.8) is used, as follows

$$R_r = \ln(V_r) = s_r \cdot \Delta t$$

$$f_r = \frac{|R_r|}{2\pi \Delta t}$$

$$\zeta_r = \sqrt{\frac{1}{1+\left(\frac{\operatorname{Im}ag(R_r)}{\operatorname{Re}al(R_r)}\right)^2}} \tag{A.15}$$

With the values of $V_r$, we can then calculate the residues $A_r^{'}$ if equation (A.7) is written as

$$\begin{bmatrix} 1 & 1 & \cdots & 1 \\ V_1 & V_2 & \cdots & V_{2N} \\ V_1^2 & V_2^2 & \cdots & V_{2N}^2 \\ \vdots & \vdots & \ddots & \vdots \\ V_1^{2N-1} & V_2^{2N-1} & \cdots & V_{2N}^{2N-1} \end{bmatrix} \begin{Bmatrix} A_1^{'} \\ A_2^{'} \\ A_3^{'} \\ \vdots \\ A_{2N}^{'} \end{Bmatrix} = -\begin{Bmatrix} h_0 \\ h_1 \\ h_2 \\ \vdots \\ h_{2N} \end{Bmatrix} \tag{A.16}$$

# Appendix B

## The Hilbert Transform

The shape of a signal that contains a rapidly oscillating component that varies slowly with time is called its "envelope". Based on the approach of the Hilbert transform, the rapid oscillations can be removed from the signal to produce the representation of the envelope.

The definition of the Hilbert transform of $x(t)$ is [4]

$$X_H(t) = \frac{1}{\pi}\int_{-\infty}^{\infty} \frac{x(\tau)}{t-\tau} d\tau \tag{B.1}$$

We can then use the Hilbert transform to calculate a new time signal from the original real signal. The transformed signal has the same amplitude and frequency content as the original signal and includes phase information that depends on the phase of the original signal. By combining two signals, the analytical signal forms as follows,

$$\overline{x(t)} = x(t) - iX_H(t) \tag{B.2}$$

where the real part is the original signal and the imaginary part is a version of the original real sequence with a 90° phase shift. The magnitude of the analytic signal is the envelope of the original time signal. When the envelope is plotted on a natural logarithm scale, the graph is a straight line. Then, the slope of the line is determined for estimating the damping ratio. The approach in detail is shown next [5][6][7].

The impulse response function of a signal-degree-of-freedom (SDOF) system can be described with the following equation

$$x(t) = Ae^{-\zeta w_n t} \sin\left(w_n \left(\sqrt{1-\zeta^2}\right) \cdot t\right) \tag{B.3}$$

where $w_n$ is the natural frequency, $\zeta$ is the damping ratio, and $A$ is the residue. The Hilbert transform of the signal is, from equation (B.1),

$$X_H(t) = Ae^{-\zeta w_n t}\cos\left(w_n\left(\sqrt{1-\zeta^2}\right)\cdot t\right) \tag{B.4}$$

The analytic signal is,

$$\overline{x(t)} = Ae^{-\zeta w_n t}\left(\sin\left(w_n\left(\sqrt{1-\zeta^2}\right)\cdot t\right) - i\cos\left(w_n\left(\sqrt{1-\zeta^2}\right)\cdot t\right)\right) \tag{B.5}$$

The magnitude of the analytic signal eliminates the oscillatory component, and gives the envelope as follows,

$$\left|\overline{x(t)}\right| = \sqrt{\left(Ae^{-\zeta w_n t}\right)^2\left(\sin^2\left(w_n\left(\sqrt{1-\zeta^2}\right)\cdot t\right) + \cos^2\left(w_n\left(\sqrt{1-\zeta^2}\right)\cdot t\right)\right)} = Ae^{-\zeta w_n t} \tag{B.6}$$

Taking the natural logarithm of each side yields,

$$\ln\left|\overline{x(t)}\right| = \ln\left(Ae^{-\zeta w_n t}\right) = \ln(A) - (\zeta w_n)\cdot t \tag{B.7}$$

This is the equation of a straight line. If the slope of the line is calculated, we can estimate the damping ratio as follows,

$$\zeta = \frac{-\,slope}{w_n} \tag{B.8}$$

# Appendix C

## The Matlab Codes

## Generating Data With Three Separated Modes

```
%#####################################################################%
%
% Project Title: Extracting Damping Ratios Using Wavelet
%
% Name: Jiun-Yan Wu
% ID: 926119127
% Date: 5/11/2001
%
% irf_1: To Generate a Simulated IRF(x) With Three Separated Modes
%           x = (A1*exp(-a1*t).*sin(wd1*t) + A2*exp(-a2*t).*sin(wd2*t) +
 A3*exp(-a3*t).*sin(wd3*t));
%
%#####################################################################%
clear;
clc;
format long g;
close all hidden;
%#####################################################################%
%
% Defining Data Parameters
%
%#####################################################################%
df = 1;
% Total Time
tt = 1/df;
% Sampling Frequency Number
L = tt*2048;
t = linspace(0,tt,L);
dt = t(3) - t(2);
N = L/2;
f = linspace(0,df*(N-1),N);
%#####################################################################%
%
% Simulating IRF Generated by Setting First Damping Ratio
%
%#####################################################################%
% First Mode
A1 = 5;
E1 = input('First Damping Ratio: ');
fn1 = df*N/8;
wn1 = fn1*2*pi;
a1 = E1*wn1;
```

```
wd1 = wn1*sqrt(1 - E1^2);
% Second Mode
A2 = 3*A1;
E2 = 2*E1;
fn2 = 2*fn1;
wn2 = fn2*2*pi;
a2 = E2*wn2;
wd2 = wn2*sqrt(1 - E2^2);
% Third Mode
A3 = 1.5*A2;
E3 = 2*E2;
fn3 = 2*fn2;
wn3 = fn3*2*pi;
a3 = E3*wn3;
wd3 = wn3*sqrt(1 - E3^2);
% Simulated IRF With Three Separate Modes
x = (A1*exp(-a1*t).*sin(wd1*t) + A2*exp(-a2*t).*sin(wd2*t) +
 A3*exp(-a3*t).*sin(wd3*t));
%#################################################################%
%
% Adding Noise Level SNR (db)
%
%#################################################################%
noise_level = menu('Select Noise Level SNR(db)','INFINITE','20','10');
if noise_level == 1
    snr=inf;
elseif noise_level == 2
    snr=20;
elseif noise_level == 3
    snr=10;
end
var_s=cov(x);
var_noise = var_s/(10^(snr/10));
n=sqrt(var_noise)*randn(length(x),1);
x=x+n';
% Calculating the Frequency Response Function (FRF)
x_ft = fft(x);
% Display Freqs. and Damping Ratios
disp('Natural Frequencies and Damping Ratios for the Data With Three Separate
 Frequencies')
Natural_Frequency_Damping_Ratio = [ fn1 E1 ; fn2 E2 ; fn3 E3]
fig =1;
p_fig = menu('Plot graphs?','Yes','No');
if p_fig == 1
%#################################################################%
%
% Graphing Data
%
%#################################################################%
figure(fig);
plot(t,x);
title(sprintf('IRF With Three Separate Frequencies'));
xlabel('Time (Seconds)');
ylabel('Real');
fig =fig+1;
figure(fig);
semilogy(f,abs(x_ft(1:N)));
title(sprintf('FRF With Three Separate Frequencies'));
```

```
xlabel('Frequency (Hz)');
ylabel('Semilog Magnitude');
end
%######################################################################%
%
% Menu for Selecting One Method to Analyze
%
%######################################################################%
method = menu('Choose Extracting Method','CEM','WPM','CWT');
if method == 1
cem_analysis
elseif method == 2
wpm_analysis
elseif method == 3
cwt_analysis
end
```

## Generating Data With Three Close Modes

```
%######################################################################%
%
% Project Title: Extracting Damping Ratios Using Wavelet
%
% Name: Jiun-Yan Wu
% ID: 926119127
% Date: 5/11/2001
%
% irf_1: To Generate a Simulated IRF(x) With Three Close Modes
%            x = (A1*exp(-a1*t).*sin(wd1*t) + A2*exp(-a2*t).*sin(wd2*t) +
 A3*exp(-a3*t).*sin(wd3*t));
%
%######################################################################%
clear;
clc;
format long g;
close all hidden;
%######################################################################%
%
% Defining Data Parameters
%
%######################################################################%
df = 1;
% Total Time
tt = 1/df;
% Sampling Frequency Number
L = tt*2048;
t = linspace(0,tt,L);
dt = t(3) - t(2);
N = L/2;
f = linspace(0,df*(N-1),N);
%######################################################################%
%
% Simulating IRF Generated by Setting First Damping Ratio
%
%######################################################################%
```

```
% First Mode
A1 = 5;
E1 = input('First Damping Ratio: ');
fn1 = df*N/4;
wn1 = fn1*2*pi;
a1 = E1*wn1;
wd1 = wn1*sqrt(1 - E1^2);
% Second Mode
A2 = 3*A1;
E2 = 1.2*E1;
fn2 = 1.2*fn1;
wn2 = fn2*2*pi;
a2 = E2*wn2;
wd2 = wn2*sqrt(1 - E2^2);
% Third Mode
A3 = 1.5*A2;
E3 = 1.3*E2;
fn3 = 1.3*fn2;
wn3 = fn3*2*pi;
a3 = E3*wn3;
wd3 = wn3*sqrt(1 - E3^2);
% Simulated IRF With Three Separate Modes
x = (A1*exp(-a1*t).*sin(wd1*t) + A2*exp(-a2*t).*sin(wd2*t) +
  A3*exp(-a3*t).*sin(wd3*t));
%######################################################################%
%
% Adding Noise Level SNR (db)
%
%######################################################################%
noise_level = menu('Select Noise Level SNR(db)','INFINITE','20','10');
if noise_level == 1
    snr=inf;
elseif noise_level == 2
    snr=20;
elseif noise_level == 3
    snr=10;
end
var_s=cov(x);
var_noise = var_s/(10^(snr/10));
n=sqrt(var_noise)*randn(length(x),1);
x=x+n';
% Calculating the Frequency Response Function (FRF)
x_ft = fft(x);
% Display Freqs. and Damping Ratios
disp('Natural Frequencies and Damping Ratios for the Data With Three Close
  Frequencies')
Natural_Frequency_Damping_Ratio = [ fn1 E1 ; fn2 E2 ; fn3 E3]
fig =1;
p_fig = menu('Plot graphs?','Yes','No');
if p_fig == 1
%######################################################################%
%
% Graphing Data
%
%######################################################################%
figure(fig);
plot(t,x);
title(sprintf('IRF With Three Close Frequencies'));
```

```
xlabel('Time (Seconds)');
ylabel('Real');
fig =fig+1;
figure(fig);
semilogy(f,abs(x_ft(1:N)));
title(sprintf('FRF With Three Close Frequencies'));
xlabel('Frequency (Hz)');
ylabel('Semilog Magnitude');
end
%######################################################################%
%
% Menu for Selecting One Method to Analyze
%
%######################################################################%
method = menu('Choose Extracting Method','CEM','WPM','CWT');
if method == 1
cem_analysis
elseif method == 2
wpm_analysis
elseif method == 3
cwt_analysis
end
```

## The Complex-Exponential Method

```
%######################################################################%
%
% Project Title: Extracting Damping Ratios Using Wavelet
%
% Name: Jiun-Yan Wu
% ID: 926119127
% Date: 5/11/2001
%
% cem_analysis: The Complex-Exponential Method
%
%######################################################################%
method = 'cem';
format long g;
%######################################################################%
%
% Defining Data Parameters
%
%######################################################################%
frf = x_ft;
N = length(frf)/2;
frf = conj(frf(1:N)');
f = f(1:N);
df = f(3) - f(2);
%######################################################################%
%
% Specifing the Frequency Range
%
%######################################################################%
specify = menu('How do you want to specify the freq. range?','Point on Graph','Type
 it');
```

```
if specify == 1
figure(fig + 1);
semilogy(f(1:N),abs(frf(1:N)));
title('Select The First Point (Minimum Frequency)');
xlabel('Frequency (Hz)');
ylabel('Semilog Magnitude');
[x_fr1,y]=ginput(1);
figure(fig + 1);
semilogy(f(1:N),abs(frf(1:N)));
title('Select The Second Point (Maximum Frequency)');
xlabel('Frequency (Hz)');
ylabel('Semilog Magnitude');
[x_fr2,y]=ginput(1);
sprintf('The Selected Frequency Range Is:\n\tMinimum freq = %8.4g\n\tMaximum
  freq = %8.4g',x_fr1,x_fr2)
else
figure(fig + 1);
semilogy(f(1:N),abs(frf(1:N)));
title('FRF');
xlabel('Frequency (Hz)');
ylabel('Semilog Magnitude');
x_fr1 = input('Minimum Frequency (Hz): ');
x_fr2 = input('Maximum Frequency (Hz): ');
sprintf('The Selected Frequency Range Is:\n\tMinimum freq = %d\n\tMaximum freq =
  %d' ,x_fr1,x_fr2)
end
%###################################################################%
%
% Isolating the Frequency Range
%
%###################################################################%
x_fr1 = round(x_fr1/df + 1);
x_fr2 = round(x_fr2/df + 1);
% Putting Zeros Before the Isolated
frf_F1 = zeros(x_fr1-1,1);
% Isolated FRF Components
frf_F1(x_fr1:x_fr2) = frf(x_fr1:x_fr2);
% Putting Zeros After the Isolated FRF Components
frf_F1(x_fr2+1:N) = ones(N-(x_fr2),1);
% Adding the Conjugate Components to the FRF
frf_F1(N+1) = real(frf_F1(N));
frf_F1(N+2:2*N) = conj(frf_F1(N:-1:2));
[r,c] = size(frf_F1);
if r <c
frf = conj(frf_F1');
else
frf = frf_F1;
end
%###################################################################%
%
% Calculating the Impulse Response Function from the FRF Inverse
%
%###################################################################%
figure(fig + 1);
semilogy(f(x_fr1:x_fr2),abs(frf(x_fr1:x_fr2)));
title(sprintf('FRF (Truncated)'));
xlabel('Frequency (Hz)');
ylabel('Semilog Magnitude');
```

```
n = input('How many DOF?: ');
irf = real(ifft(frf));
% Time parameters
t = linspace(0,1/df,2*N);
dt = t(2)-t(1);
%#####################################################################%
%
% Processing Data
%
%#####################################################################%
L = length(irf);
M = L/2;
n=n*2;
for r = 1:n
h1(:,r) = real(irf(r:M-1+r));
end
for r = 1:M
hv1(r,:) = -real(irf(n+r));
end
B1 = inv(h1'*h1)*(h1'*hv1);
B1(n+1,1) = 1;
B1v = B1(n+1:-1:1);
V_cem = roots(B1v);
% Calculating the Natural Freq & Damping Ratio
n = length(V_cem);
for r = 1:n
wn_cem(r) = abs(log(V_cem(r)))/dt;
Fn_cem(r) = wn_cem(r)/(2*pi);
Damp_ratio_cem(r) = sqrt(1/(((imag(log(V_cem(r)))/real(log(V_cem(r))))^2)+1));
end
% Calculating eigenvector
for r = 0:(2*N - 1)
Va_cem(r+1,:) = [conj(V_cem').^r ];
end
Ar_cem = (inv(conj(Va_cem')*Va_cem)*conj(Va_cem')*(irf));
% Calcualting the IRF Curve Fit
x_cem = Va_cem*Ar_cem;
% Calcualting the FRF Curve Fit
frf_cem = fft(x_cem);
%#####################################################################%
%
% Graphing Data
%
%#####################################################################%
figure(fig + 2);
semilogy(f(x_fr1:x_fr2),abs(frf(x_fr1:x_fr2)),'-',f(x_fr1:x_fr2),abs(frf_cem(x_fr1:x_fr
 2)),':');
title(sprintf('FRF'));
xlabel('Frequency (Hz)');
ylabel('Semilog Magnitude');
legend('Simulated Curve','Curve Fit',0)
figure(fig + 3);
plot(f(x_fr1:x_fr2)',angle(frf(x_fr1:x_fr2)),'-',f(x_fr1:x_fr2)',angle(frf_cem(x_fr1:x_fr
 2)),':');
title(sprintf('Phase Angle'));
xlabel('Frequency (Hz)');
ylabel('Phase Angle (Radians)');
legend('Simulated Curve','Curve Fit',0)
```

```
figure(fig + 4);
plot(t,irf,'-',t,real(x_cem),':');
title(sprintf('IRF'));
xlabel('Time (Seconds)');
ylabel('Real');
legend('Simulated Curve','Curve Fit',0)
%######################################################################%
%
% Displaying Result
%
%######################################################################%
Natural_freq_Damping_ratio_cem = [ Fn_cem' Damp_ratio_cem' ]
```

## The Wavelet Packet Method

```
%######################################################################%
%
% Project Title: Extracting Damping Ratios Using Wavelet
%
% Name: Jiun-Yan Wu
% ID: 926119127
% Date: 5/11/2001
%
% wpm_analysis: The Wavelet Packet Method
%
%######################################################################%
method = 'wpm';
x_ori=x;
format long g;
%######################################################################%
%
% Defining Data Parameters
%
%######################################################################%
wname='coif5';
l = input('Enter Decomposition Level: ');
% Decomposing IRF Using 'wname' by l Level
[th d]=wpdec(x,l,wname);
m=power(2,l);
node = zeros(m,2048);
%######################################################################%
%
% Visualizing FRF for Each Node (Denoted From Node 1 to Node 2^Level)
%
%######################################################################%
% Reconsturcting IRF for Each Node From its Coeffs.
for k=1:m
    node(k,:)=wprcoef(th,d,[l k-1]);
end
% Graphing FRF for Nodes
for k=1:m/2
    x_dft_1=fft(node(2*k-1,:));
    x_dft_2=fft(node(2*k,:));
    fig=fig+k;
    figure(fig);
    subplot(2,1,1);
    semilogy(f,abs(x_dft_1(1:N))); ax=gca;
```

```
    axTITL=get(ax,'title');
    str1=['Node' num2str(2*k-1)];
    set(axTITL,'String',str1);
    xlabel('Frequency (Hz)');
    ylabel('Semilog Magnitude');
    subplot(2,1,2);
    semilogy(f,abs(x_dft_2(1:N)));ax=gca;
    axTITL=get(ax,'title');
    str1=['Node' num2str(2*k)];
    set(axTITL,'String',str1);
    xlabel('Frequency (Hz)');
    ylabel('Semilog Magnitude');
end
%##################################################################%
%
% Processing Data
%
%##################################################################%
n = input('How many DOF ?');
wpm=zeros(n,2048);
abswmp=zeros(n,2048);
logwmp=zeros(n,2048);
x_wpm=zeros(1,2048);
for k=1:n
    index='a';
     disp('Reconstruct Each Mode by Analysing FRF');
        while (index ~= 'q')
            disp('Choose Node Number: For Example by Typing node(3,:) for Node3 ');
            add=input('');
            wpm(k,:)=wpm(k,:)+add;
            index=input('-----Add "a" or Quit "q"-----');
        end
        x_wpm=x_wpm+wpm(k,:);
        frf_wpm=fft(x_wpm);
% Performing Hilbert Transform to get the Envelop Function
abswmp(k,:)=abs(hilbert(wpm(k,:)));
fig=fig+1;
figure(fig);
plot(t,abswmp(k,:));
title('Envelop Function for Each Mode by Performing Hilbert Transform');
xlabel('Time (Seconds)');
ylabel('Amplitude (Units)');
% Performing Natural Logarithm to get the Straight Line
logwmp(k,:)=log(abswmp(k,:));
fig=fig+1;
figure(fig);
plot(t,logwmp(k,:));
title('Select Two Points in the Time Domain (X Axis)');
xlabel('Time (Seconds)');
ylabel('Log-Amplitude (Units)');
[x,y]=ginput(2);
sprintf('The Selected Time Range Is:\n\tMinimum Time: %8.5g \n\tMaximum Time:
 %8.5g',x(1),x(2))
%##################################################################%
%
% Least Square Method to Calculate Slope, and Then Damping Ratio
%
%##################################################################%
```

```
[np] = round(x/dt + 1);
t1 = t(np(1):np(2));
% Calculates the Amount of Points Data
m = length(t1);
temp=logwmp(k,np(1):np(2));
% Summatory of the t points (x components)
sum_x = sum(t1);
% Summatory of the env_dB points (y components)
sum_y = sum(temp);
% Summatory of the square value of each t points (x components)
sum_x_sq = dot(t1,t1);
% Summatory of the multiplication of t and env_dB points (x and y components)
sum_xy = dot(t1,temp);
LQ1 = [m sum_x; sum_x sum_x_sq];
LQ2 = [sum_y ; sum_xy];
LQ3 = inv(LQ1) * LQ2;
slope(k) = LQ3(2);
end
Damp_ratio_wpm(1)=-slope(1)/wn1;
Damp_ratio_wpm(2)=-slope(2)/wn2;
Damp_ratio_wpm(3)=-slope(3)/wn3;
%####################################################################%
%
% Graphing Data
%
%####################################################################%
figure(fig + 1);
semilogy(f,abs(x_ft(1:N)),'-',f,abs(frf_wpm(1:N)),':');
title(sprintf('FRF'));
xlabel('Frequency (Hz)');
ylabel('Semilog Magnitude');
legend('Simulated Curve','Curve Fit',0)
figure(fig + 2);
plot(t,x_ori,'-',t,real(x_wpm),':');
title(sprintf('IRF'));
xlabel('Time (Seconds)');
ylabel('Real');
legend('Simulated Curve','Curve Fit',0)
%####################################################################%
%
% Displaying Result
%
%####################################################################%
Damping_Ratio_WPM = [Damp_ratio_wpm' ]
```

## The Continuous Wavelet Transform Method

```
%####################################################################%
%
% Project Title: Extracting Damping Ratios Using Wavelet
%
% Name: Jiun-Yan Wu
% ID: 926119127
% Date: 5/11/2001
%
```

```
% cwt_analysis: The Continuous Wavelet Transform Method
%
%#####################################################################%
method = 'cwt';
format long g;
%#####################################################################%
%
% Defining Data Parameters
%
%#####################################################################%
wname   = 'cmor1-1.5';
A = 0; B = 1; P = 2048;
t = linspace(A,B,P);
delta = (B-A)/(P-1);
%#####################################################################%
%
% Calculating Scales to Frequencies
%
%#####################################################################%
scales = [1:1:60];
tab_PF = scal2frq(scales,wname,delta);
n = input('How many DOF?: ');
for k=1:n
  sprintf('Type Natural Frequency (Hz) for Mode %d',k)
  tab_FREQ(k)=input('');
  [dummy,ind] = min(abs(tab_PF-tab_FREQ(k)));
  PF_app(k) = tab_PF(ind);
  SC_app(k) = scales(ind);
end
Corres_Scale_to_Pseudo_Freq = [SC_app' PF_app' ]
%#####################################################################%
%
% Processing Data
%
%#####################################################################%
coeffs=cwt(x,scales,wname,'plot'); ax = gca; colorbar
% Set Zeros Matrix
c=zeros(60,2048);
absc=zeros(60,2048);
logc=zeros(60,2048);
for k=1:n
    c(k,:)=coeffs(SC_app(k),:);
    absc(k,:)=abs(c(k,:));
    logc(k,:)=log(absc(k,:));
end
%#####################################################################%
%
% Graphing Data
%
%#####################################################################%
for k=1:n
figure(fig + k*2-1);
plot(t,absc(k,:));
title(sprintf('Coeffs of CWT with Dilation Corresponding to the Analysed
 Frequency-Absolute Value'));
xlabel('Time (Seconds)');
ylabel('Amplitude (Units)');
figure(fig + k*2);
```

```
plot(t,logc(k,:));
title('Select Two Points in the Time Domain (X Axis)');
xlabel('Time (Seconds)');
ylabel('Log-Amplitude (Units)');
[x,y]=ginput(2);
sprintf('The Selected Time Range Is:\n\tMinimum Time: %8.5g \n\tMaximum Time:
 %8.5g',x(1),x(2))
%####################################################################%
%
% Least Square Method to Calculate Slope, and Then Damping Ratio
%
%####################################################################%
[np] = round(x/dt + 1);
t1 = t(np(1):np(2));
% Calculates the Amount of Points Data
m = length(t1);
temp=logc(k,np(1):np(2));
% Summatory of the t points (x components)
sum_x = sum(t1);
% Summatory of the env_dB points (y components)
sum_y = sum(temp);
% Summatory of the square value of each t points (x components)
sum_x_sq = dot(t1,t1);
% Summatory of the multiplication of t and env_dB points (x and y components)
sum_xy = dot(t1,temp);
LQ1 = [m sum_x; sum_x sum_x_sq];
LQ2 = [sum_y ; sum_xy];
LQ3 = inv(LQ1) * LQ2;
slope(k) = LQ3(2);
end
Damp_ratio_cwt(1)=-slope(1)/wn1;
Damp_ratio_cwt(2)=-slope(2)/wn2;
Damp_ratio_cwt(3)=-slope(3)/wn3;
%####################################################################%
%
% Displaying Result
%
%####################################################################%
Natural_Freq_Damping_Ratio_CWT = [ PF_app' Damp_ratio_cwt' ]
```

# List of References

[1] M. Paz. Structural Dynamics: Theory and Computation. $2^{nd}$ Ed. Van Nostrand Reinhold Company, 1985.

[2] N. Manuel Mendes Maia and J. Montalvao. Theoretical and Experimental Modal Analysis. John Wiley & Sons Inc., New York, 1997.

[3] Angel Moises Iglesias. Investigating various modal analysis extraction techniques to estimate damping ratio. M.S. Project, Virginia Polytechnic Institute and State University, 2000.

[4] M. Feldman. Non-linear system vibration analysis using Hilbert transform-I. free vibration analysis method 'FREEVIB'. Mechanical Systems and Signal Processing, 8(2): 119-127, 1994.

[5] M. Ruzzene, A. Fasana, L. Garibaldi and B. Piombo. Natural frequencies and dampings identification using wavelet transform: application to real data. Mechanical Systems and Signal Processing, 11(2): 207-218, 1997.

[6] W. J. Staszewski. Identification of damping in MDOF systems using time-scale decomposition. Journal of Sound Vibration, 203(2): 283-305, 1997.

[7] B. A. D. Piombo, A. Fasana, S. Marchesiello and M. Ruzzene. Modelling and identification of the dynamic response of a supported bridge. Mechanical Systems and Signal Processing, 14(1): 75-89, 2000.

[8] S. Mallat. A Wavelet Tour of Signal Processing. $2^{nd}$ Ed. Courant Institute, New York University, 1998.

[9] R. M. Rao and A. S. Bopardikar. Wavelet Transforms: Introduction to Theory and

Applications. Addison Wesley Longman Inc., 1998.

[10] The Math Works Inc. Wavelet ToolBox User's Guide, Version 1, March 1996.

[11] K. P. L. Veroy. Time-frequency analysis of lamb waves using the Morlet wavelet transform. M.S. Project, Massachusetts Institute of Technology, 2000.

[12] W. J. Staszewski and G. R. Tomlinson. Application of the wavelet transform to fault detection in a spur gear. Mechanical Systems and Signal Processing, 8(3): 289-307, 1994.